



Stability analysis for the phytoplankton-zooplankton model with depletion of dissolved oxygen and strong Allee effects

Ahmed Ali^a, Shireen Jawad^a, Ali Hasan Ali^{b,c,*}, Matthias Winter^d

^a Department of Mathematics, College of Science, University of Baghdad, Baghdad, 10071, Iraq

^b Institute of Mathematics, University of Debrecen, Pf. 400, H-4002, Debrecen, Hungary

^c Jadara University Research Center, Jadara University, Irbid 21110, Jordan

^d Department of Mathematics, Brunel University London, Uxbridge, UB8 3PH, UK

ARTICLE INFO

MSC:
2020: 34D05
34D20
34D23
34D45
92D40
92D25

Keywords:
Plankton interaction
Strong Allee effect
Dissolved oxygen
Stability analysis
Hopf bifurcation

ABSTRACT

The photosynthetic activity of phytoplankton in the seas is responsible for an estimated 50–80 % of the world's oxygen generation. Both phytoplankton and zooplankton require some of this synthesized oxygen for cellular respiration. This study aims to better understand how the oxygen-phytoplankton dynamics are altered due to the Allee effect in phytoplankton development, particularly when considering the time-dependent oxygen generation rate. The dynamic analysis of the model is dedicated to finding the possible equilibrium points. The analysis reveals that three equilibrium points can be obtained. The stability study demonstrates that one of the equilibrium points is always stable. The remaining equilibrium points are stable under specific conditions. We also identify bifurcations originating from these equilibrium points, including transcritical, pitchfork, and Hopf bifurcation. We derive conditions for stable limit cycles (supercritical Hopf bifurcation) and, in some cases, establish the non-existence of solutions. Numerical simulations are performed to validate our theoretical findings. Furthermore, it is noted that the Allee threshold for the phytoplankton population (k_0) significantly influences the overall dynamics of the system. When $k_0 \leq 0.001$, the population of plankton is at risk of extinction. On the other hand, when $0.001 < k_0 \leq 0.01$, the population of zooplankton is at risk of extinction. When $0.01 < k_0 \leq 2$, the solution reaches a stable condition of coexistence. Conversely, when $k_0 \geq 2.1$, the solution exhibits periodic attractor behaviour.

1. Introduction

Understanding dissolved oxygen dynamics has received much interest because it is such a key indicator for the health of the marine ecosystem [1–3]. Phytoplankton, the planktonic communities most resembling plants, supply the vast majority of the oxygen in the oceans through photosynthesis and serve as the foundation of the marine food chain. It is commonly known that the amount of oxygen generated by phytoplankton varies significantly due to environmental fluctuations such as the rate of salinity, the level of temperature, and the number of nutrients. Further, phytoplankton's oxygen production varies dramatically throughout the day and night. Therefore, the link between phytoplankton and dissolved oxygen is essential to the survival of most species, from the simplest (a single cell) to the most sophisticated (a human being). Changes in oxygen production can have profound consequences for marine life [4]. For instance, some environmental factors,

including temperature, affect phytoplankton's biomass and growth. Dissolved oxygen levels in water fluctuate on a daily cycle since oxygen is created during photosynthesis (during the day) and absorbed during respiration (at all times). Phytoplankton communities are, therefore, valuable indicators of environmental changes [5–8]. For example, Mondal, Samanta and De la Sen have investigated how the coupled plankton-oxygen dynamics in the ocean is affected by a low oxygen production rate which can lead to oxygen depletion and plankton extinction [9].

Most modelers generally select the Logistic growth form as the growth function for the prey species without considering the predator species [10–12]. However, it is common knowledge that the resources available in an ecosystem, such as space, food, and the components of essential nutrition, are finite. As the population grows, the average growth rate steadily decreases. The average growth rate drops to zero as the population meets the environment's carrying capacity, k , and drops

* Corresponding author.

E-mail address: ali.hasan@science.unideb.hu (A.H. Ali).

<https://doi.org/10.1016/j.rineng.2024.102190>

Received 29 October 2023; Received in revised form 20 April 2024; Accepted 26 April 2024

Available online 3 May 2024

2590-1230/© 2024 The Authors. Published by Elsevier B.V. This is an open access article under the CC BY-NC-ND license (<http://creativecommons.org/licenses/by-nc-nd/4.0/>).

further for any population size greater than k . Further, a substantial body of research suggests that a low population density actually has the opposite effect. The Allee effect is the name of this phenomenon, which describes the positive density dependency of population increase in areas with low densities [13].

On the other hand, the study of theoretical ecology has as its primary goal the identification of the various dynamical mechanisms linked with interactions between prey and predator [14–16]. An example of a particular type of predator-prey interaction that opens up various facets of marine ecology is the relationship between phytoplankton and zooplankton. Phytoplankton significantly contributes to aquatic ecosystems, including producing an enormous amount of oxygen, managing natural resources and water quality, and providing the basis for various food webs [17,18]. Research on the dynamics of plankton is a fascinating topic. The building blocks of all aquatic food chains can be found in plankton, with phytoplankton occupying the first trophic level of the food chain [19]. Phytoplankton toxins play a critical environmental function and can not be disregarded. Environmental stress factors, optimal environmental circumstances, nutrient-limited settings, and other similar characteristics are significant contributors to the release of toxins. Some phytoplankton species are notorious for producing and releasing toxic or allelochemicals into the environment, which can be detrimental to other plankton species [20]. For instance, Venturino, Chattopadhyay and their colleagues have demonstrated that toxin-producing phytoplankton works as a controlling agent for the cessation of plankton blooms [21]. Dhar and Baghel consider the effect of dissolved oxygen on the presence of an interacting planktonic population. They conclude that the possibility of Hopf-bifurcation in the interior equilibrium could occur if the phytoplankton growth rate is chosen as the bifurcation parameter [22].

The objective of this research is to investigate the dynamics of the oxygen-plankton model as a result of the combined influence of the Allee effect on the growth of phytoplankton and the time-dependent oxygen production rate in particular. Considering these effects, we propose a DOPZ model of dissolved oxygen-phytoplankton- zooplankton interaction with a strong Allee effect on phytoplankton growth. This paper's findings provide additional context for [22] by.

- Replacing the linear form in the growth rate of the phytoplankton population with growth in the form of the strong Allee effect.
- In addition, our model includes both toxic and non-toxic phytoplankton, and we assume the zooplankton consumes both.
- Further, we consider that some phytoplankton species have a low chance of being eaten by zooplankton by hiding in the various sediments on the seafloor. These sediments provide the prey with a place to hide from their predators.
- Finally, since the phytoplankton performs photosynthesis throughout the day, they release oxygen into the atmosphere. This phenomenon has been considered in our model.

After presenting the construction of our model, then our goal is to observe the impact of the Allee threshold on the dynamics of a DOPZ model. In addition, the comprehension of the nonlinear dynamics of our model will be discussed by employing different methodologies such as stability and bifurcation analysis techniques. Finally, we will verify the accuracy of our analytical results by simulating the proposed system numerically.

2. Construction of the model

Our work involves a 3D model of an aquatic system with three components: phytoplankton $u(t)$, zooplankton $v(t)$, and concentration of dissolved oxygen $w(t)$. The following presumptions form the basis of the mathematical model that will aid in our understanding of the dynamics of the DOPZ system.

The phytoplankton population is assumed to come in two types, toxic

and non-toxic which can occasionally release harmful substances [23]. Phytoplankton species are assumed to grow according to the strong Allee effect type of growth. The term $\frac{ru}{(a_1+w_0-w)} \left(1 - \frac{u}{k}\right) \left(\frac{u}{k_0} - 1\right)$ stands for the Allee effect type growth of phytoplankton, combining the absorption of dissolved oxygen with the growth rate r , the maximal phytoplankton carrying capacity k and the critical phytoplankton level k_0 (Allee threshold) such that $0 < k_0 < k$ [11]. When the population density drops below the critical threshold k_0 , the population starts to decrease, and the population tends to extinction. w_0 is the constant concentration of dissolved oxygen that comes from several sources in the water; a_1 is the phytoplankton saturation constant; δ_1 denotes the phytoplankton's natural death rate; $a_1 u(1-m)v$ represents the predation of the available phytoplankton by zooplankton. In addition, we consider that some phytoplankton populations have a low chance of being eaten by zooplankton by hiding in the various sediments that may be found on the seafloor. These sediments provide the prey with a place to hide from their predators [24]. Hence, $(1-m)$ represents the proportion of unprotected phytoplankton consumed by various zooplankton types. Thus the phytoplankton equation has the following form:

$$\frac{du}{dt} = \frac{ru}{(a_1+w_0-w)} \left(1 - \frac{u}{k}\right) \left(\frac{u}{k_0} - 1\right) - a_1 u(1-m)v - \delta_1 u.$$

It is assumed that zooplankton feeds on the two categories mentioned above according to a modified Holling type I and II response [22,25]. Thus, $\frac{a_2 u(1-m)v}{(a_2+w_0-w)}$ denotes the conversion from phytoplankton to zooplankton; a_2 is the zooplankton saturation constant; $au(1-m)v$ stands for the predation of toxic phytoplankton by zooplankton; δ_2 represents the zooplankton's natural death rate. Therefore, the equation of zooplankton species can be written as

$$\frac{dv}{dt} = \frac{a_2 u(1-m)v}{(a_2+w_0-w)} - \delta_2 v - au(1-m)v.$$

$w(t)$ represents the oxygen concentration in an aquatic environment. Further, since the phytoplankton performs photosynthesis throughout the day, they release oxygen into the atmosphere. Additionally, the rate of oxygen depletion can be attributed to various factors, including the consumption of oxygen by phytoplankton during the night, the respiration of marine animals, and the gradual decline in oxygen concentration that results from chemical reactions that take place in the water [26]. Thus, $s(w_0 - w)$ represents the dissolved oxygen concentration that comes from other sources, du represents the amount of oxygen produced as a result of the process of photosynthesis carried out by phytoplankton. $\gamma_1 uw$ is the consumption of oxygen by phytoplankton during the night. $\gamma_2 vw$ denotes the consumption of oxygen by zooplankton. γ is the natural depletion rate of oxygen. In this case, the dissolved oxygen equation can be written as:

$$\frac{dw}{dt} = s(w_0 - w) + du - \gamma w - \gamma_1 uw - \gamma_2 vw.$$

The following set of ordinary differential equations serves as the governing structure for the dynamical system of the DOPZ model:

$$\begin{aligned} \frac{du}{dt} &= \frac{ru}{(a_1 + w_0 - w)} \left(1 - \frac{u}{k}\right) \left(\frac{u}{k_0} - 1\right) - a_1 u(1-m)v \\ &- \delta_1 u = f_1(u, v, w), \frac{dv}{dt} = \frac{a_2 u(1-m)v}{(a_2 + w_0 - w)} - \delta_2 v \\ &- au(1-m)v = f_2(u, v, w), \frac{dw}{dt} = s(w_0 - w) + du - \gamma w - \gamma_1 uw \\ &- \gamma_2 vw = f_3(u, v, w) \end{aligned} \quad (1)$$

with the initial conditions $u(0) = u_0 \geq 0$, $v(0) = v_0 \geq 0$. All parameters for the dissolved oxygen-phytoplankton-zooplankton model (DOPZ) are expected to be positive and clarified in Table 1.

Further, Fig. 1 illustrates the schematic sketch of the DOPZ model.

In addition, the equations of the DOPZ model are $C^1(R_+^3)$, where $R_+^3 = \{(u, v, w), u \geq 0, v \geq 0, w \geq 0\}$. Therefore, they can be represented as Lipschitzian [27]. Thus, the solution of the DOPZ model exists, and it is unique.

Table 1

The biological interpretation of the DOPZ system's parameters.

Parameters	Biological interpretation
r	The growth rate of phytoplankton.
α_1	The capture rate of the available non-toxic phytoplankton by zooplankton.
$m \in (0, 1)$	The proportion of protected phytoplankton.
α_2	The conversion rate from phytoplankton to zooplankton.
a	The predation rate of toxic phytoplankton by zooplankton.
δ_1	The phytoplankton's natural death rate.
δ_2	The zooplankton's natural death rate.
a_1	The phytoplankton saturation constant.
a_2	The zooplankton saturation constant.
w_0	The constant concentration of dissolved oxygen that comes from other sources.
s	The replenishment rate of oxygen in the marine.
d	The amount of oxygen produced as a result of the process of photosynthesis carried out by phytoplankton.
γ	The natural depletion rate of oxygen.
γ_1	The consumption of oxygen by phytoplankton during the night.
γ_2	The consumption of oxygen by zooplankton.

3. Dynamical evaluation results

In this section, the well-posedness of the system and present conclusions about the presence of potential equilibrium points are discussed. In addition, the analysis of stability and bifurcation around the potential equilibrium points is examined.

$$dw = \begin{bmatrix} sw_0 + du_{00} e^{\int_0^t \left[\frac{r}{(a_1 + w_0 - w(\tau))} \left(1 - \frac{u(\tau)}{k} \right) \left(\frac{u(\tau)}{k_0} - 1 \right) - \alpha_1 (1-m)v(\tau) - \delta_1 \right] d\tau} \\ -w \left(s + \gamma + cv\gamma_1 u_{00} e^{\int_0^t \left[\frac{r}{(a_1 + w_0 - w(\tau))} \left(1 - \frac{u(\tau)}{k} \right) \left(\frac{u(\tau)}{k_0} - 1 \right) - \alpha_1 (1-m)v(\tau) - \delta_1 \right] d\tau} \right. \\ \left. - \gamma_2 v_{00} e^{\int_0^t \left[\frac{\alpha_2 (1-m)u(\tau)}{(a_2 + w_0 - w(\tau))} - \delta_2 - a(1-m)u(\tau) \right] d\tau} \right) \end{bmatrix} dt.$$

3.1. Positivity and boundedness

Since we are working with a biological system, the solutions of the DOPZ are essential to be both positive and bounded. The boundedness of solutions indicates that none of the populations exhibit unlimited growth. The quality of being bound is a crucial aspect of the system's proper functioning, as available resources limit it.

Theorem 1. All solutions of the DOPZ model $u(t)$, $v(t)$ and $w(t)$ with the initial conditions $(u_{00}, v_{00}, w_{00}) \in R_+^3$ are positively invariant.

Proof: By integrating the first and second functions of the DOPZ model for $u(t)$ and $v(t)$ with a positive initial condition (u_{00}, v_{00}, w_{00}) , we obtain

$$u(t) = u_{00} \exp \left\{ \int_0^t \left[\frac{r}{(a_1 + w_0 - w(\tau))} \left(1 - \frac{u(\tau)}{k} \right) \left(\frac{u(\tau)}{k_0} - 1 \right) - \alpha_1 (1-m)v(\tau) - \delta_1 \right] d\tau \right\}.$$

$$v(t) = v_{00} \exp \left\{ \int_0^t \left[\frac{\alpha_2 (1-m)u(\tau)}{(a_2 + w_0 - w(\tau))} - \delta_2 - a(1-m)u(\tau) \right] d\tau \right\}.$$

Then,

$$dw = (sw_0 + du - w(s + \gamma + \gamma_1 u + \gamma_2 v))dt.$$

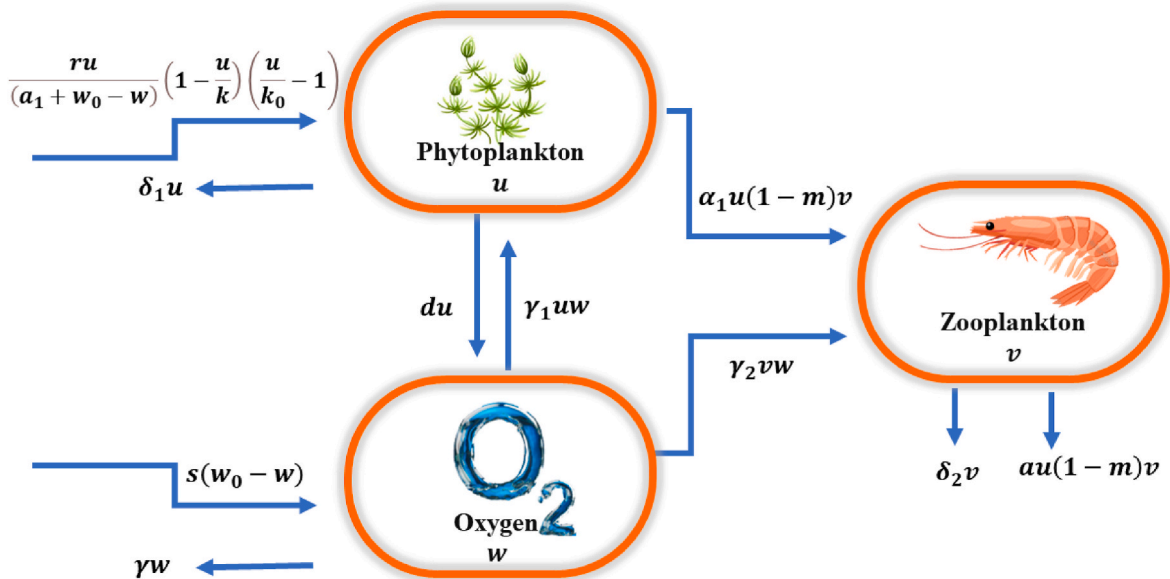


Fig. 1. Schematic diagram of the DOPZ model.

Therefore, after eliminating the non-negative terms, this produces

$$dw \geq \left[- \left(s + \gamma + \gamma_1 u_{00} e^{\int_0^t \left[\frac{r}{(a_1 + w_0 - w(\tau))} \left(1 - \frac{u(\tau)}{k} \right) - \alpha_1 (1-m)v(\tau) - \delta_1 \right] d\tau} \right) \right. \\ \left. + \gamma_2 v_{00} e^{\int_0^t \left[\frac{a_2 (1-m)u(\tau)}{(a_2 + w_0 - w(\tau))} - \delta_2 - a(1-m)u(\tau) \right] d\tau} \right] dt. \text{Consequently, by integrating the equation shown above for } w(t), \text{ these yields}$$

$$w(t) \geq w_{00} \exp \left\{ \int_0^t \left[- \left(s + \gamma + \gamma_1 u_{00} e^{\int_0^{\tau} \left[\frac{r}{(a_1 + w_0 - w(\tau))} \left(1 - \frac{u(\tau)}{k} \right) - \alpha_1 (1-m)v(\tau) - \delta_1 \right] d\tau} \right) \right. \right. \\ \left. \left. + \gamma_2 v_{00} e^{\int_0^{\tau} \left[\frac{a_2 (1-m)u(\tau)}{(a_2 + w_0 - w(\tau))} - \delta_2 - a(1-m)u(\tau) \right] d\tau} \right] d\tau \right\}.$$

As a result of the exponential function's definition, any solution, any solution $(u(t), v(t), w(t))$ that starts inside of R_+^3 with positive initial conditions (u_{00}, v_{00}, w_{00}) will remain in R_+^3 . \square

Theorem 2. Assume that $\alpha_1 \geq \alpha_2 + a$, then all solutions $u(t), v(t)$ and $w(t)$ of the DOPZ model that initiates in $\zeta = \{(u, v, w) \in R_+^3, u + v \leq \frac{kr(k+k_0)}{\delta k_0}, w \leq \frac{sw_0 + kd}{s+\gamma}\}$, where $\delta = \min\{\delta_1 + r, \delta_2\}$, are uniformly bounded.

Proof: From the last equation of the DOPZ model, we obtain.

$\frac{dw}{dt} \leq sw_0 + kd - (s + \gamma)w$, where k is the maximal phytoplankton carrying capacity. Now, by applying the separation of variables method, the following is obtained:

$$0 \leq w(t) \leq \frac{sw_0 + kd}{s+\gamma} (1 - e^{-(s+\gamma)t}) + w(0)e^{-(s+\gamma)t}.$$

Hence,

$$0 \leq \limsup_{t \rightarrow \infty} w(t) \leq \frac{sw_0 + kd}{s+\gamma} = \mathcal{J}..$$

Let $L = u + v$, then

$$\frac{dL}{dt} = \frac{du}{dt} + \frac{dv}{dt}.$$

Using the above dissolved oxygen bound and the fact that $\alpha_1 \geq \alpha_2 + a$, the following is obtained

$$\frac{dL}{dt} \leq \frac{ru}{(a_1 + w_0 - \mathcal{J})} \left(1 - \frac{u}{k} \right) \left(\frac{u}{k_0} - 1 \right) - \alpha_1 u(1-m)v - \delta_1 u + \frac{a_2 u(1-m)v}{(a_2 + w_0 - \mathcal{J})} - \delta_2 v - \text{aav}(1-m).$$

i.e.,

$$\frac{dL}{dt} \leq \frac{ru}{(a_1 + w_0 - \mathcal{J})} \left(1 - \frac{u}{k} \right) \left(\frac{u}{k_0} - 1 \right) - \delta_1 u - \delta_2 v.$$

By using the maximal phytoplankton carrying capacity k the following is obtained:

$$\frac{dL}{dt} \leq \frac{kr(k+k_0)}{k_0} - (\delta_1 + r)u - \delta_2 v.$$

$\frac{dL}{dt} + \delta L \leq \frac{kr(k+k_0)}{k_0}$, where $\delta = \min\{\delta_1 + r, \delta_2\}$. Then applying Gronwall's inequality [28], the following is obtained:

$$0 \leq L(u(t), v(t)) \leq \frac{kr(k+k_0)}{\delta k_0} (1 - e^{-\delta t}) + L(0)e^{-\delta t},$$

hence,

$$0 \leq \limsup_{t \rightarrow \infty} L(t) \leq \frac{kr(k+k_0)}{\delta k_0}.$$

So, $u(t), v(t)$ and $w(t)$ will remain bounded. \square

Remark 1. Since α_1 indicates phytoplankton depletion owing to zooplankton intake and α_2 and a represent growth and the predation rate of toxic phytoplankton due to plankton interaction respectively, it is logical to conclude that

$$\alpha_1 \geq \alpha_2 + a.$$

Since we are dealing with a nonlinear system it is not easy to solve the proposed system directly. So the better way to understand the behavior of a non-linear system is to study the stability and the possible accruing of a bifurcation near the possible equilibrium points [29].

3.2. Existence of equilibria

The DOPZ model has the following steady states.

1. The dissolved oxygen equilibrium point (DOEP) is given by $F_1 = (0, 0, \hat{w})$, where $\hat{w} = \frac{sw_0}{s+\gamma}$.
2. The zooplankton free equilibrium point (ZFEP) given by $F_2 = (\bar{u}, 0, \bar{w})$, where $\bar{w} = \frac{sw_0 + d\bar{u}}{s+\gamma+\gamma_1\bar{u}} > 0$ and \bar{u} is the root of the following equation:

$$g(u) = A_1 u^3 + A_2 u^2 + A_3 u + A_4,$$

where $A_1 = \gamma_1 r$; $A_2 = r(s + \gamma) - \gamma_1 r(k + k_0)$;

$A_3 = -r(k + k_0)(s + \gamma) - \delta_1 k k_0 d + k k_0 \gamma_1 (s a_1 + s w_0 + r)$;

$A_4 = k k_0 [(r + \delta_1 a_1)(s + \gamma) + \delta_1 w_0 \gamma]$.

Clearly, $g(0) = k k_0 [(r + \delta_1 a_1)(s + \gamma) + \delta_1 w_0 \gamma] > 0$, and

$g(k) = r^2(r(\gamma + s) - r\gamma_1(k + k_0)) - r(r(k + k_0)(\gamma + s) - k k_0 \gamma_1(r + s a_1 + s w_0) + d k k_0 \delta_1) + r^4 \gamma_1 + k k_0((\gamma + s)(r + a_1 \delta_1) + \gamma \delta_1 w_0)$.

Therefore, by the intermediate value theorem [30], $g(u)$ has a positive root say $u = \bar{u}$ in the interval $(0, k)$ if $g(k) < 0$.

3. The coexisting equilibrium point (CEP) given by $F_3 = (u^*, v^*, w^*)$, where $u^* = \frac{\delta_2(a_2 + w_0 - w^*)}{(1-m)(a_2 - a(a_2 + w_0 - w^*))}$, $v^* = \frac{r(k+k_0)u^* - r k k_0 - \delta_1 k k_0(a_1 + w_0 - w^*)}{a_1(1-m)(a_1 + w_0 - w^*) k k_0}$, and w^* is the root of the following equation:

$$B_0 w^5 + B_1 w^4 + B_2 w^3 + B_3 w^2 + B_4 w + B_5 = 0 \quad (2)$$

where, $B_i, i = 1, 2, 3, 4, 5$ are listed in the Appendix section. Using Descartes's rule of sign [31], Equation (2) has a unique positive root, if one of the following sets conditions hold:

$$B_0 > 0 \text{ and } B_{2,3,4,5} < 0, B_{0,1} > 0 \text{ and } B_{3,4,5} < 0, B_{0,1,2} > 0 \text{ and } B_{4,5} < 0, B_{0,1,2,3} > 0 \text{ and } B_5 < 0, B_0 < 0 \text{ and } B_{2,3,4,5} > 0, B_{0,1} < 0 \text{ and } B_{3,4,5} > 0, B_{0,1,2} < 0 \text{ and } B_{4,5} > 0, B_{0,1,2,3} < 0 \text{ and } B_5 > 0 \quad (3)$$

For u^* and v^* to be positive, the following two conditions must be satisfied:

$$\alpha_2 > a(a_2 + w_0 - w^*), r(k + k_0)u^* > r u^{*2} + r k k_0 + \delta_1 k k_0(a_1 + w_0 - w^*) \quad (4)$$

3.3. Local stability

The feature of the eigenvalues of the Jacobian matrix $J(u, v, w)$ at an equilibrium point is directly related to the behaviour of the DOPZ model near an equilibrium [32]. The $J(u, v, w)$ of the DOPZ model at any point, say (u, v, w) , can be written as:

$$J = \begin{bmatrix} \frac{\partial f_1}{\partial u} & \frac{\partial f_1}{\partial v} & \frac{\partial f_1}{\partial w} \\ \frac{\partial f_2}{\partial u} & \frac{\partial f_2}{\partial v} & \frac{\partial f_2}{\partial w} \\ \frac{\partial f_3}{\partial u} & \frac{\partial f_3}{\partial v} & \frac{\partial f_3}{\partial w} \end{bmatrix} = (a_{ij})_{3 \times 3}, \text{ where, } a_{11} = \frac{2ru(k+k_0) - 3ru^2 - rk k_0}{(a_1 + w_0 - w)^2 k^2 k_0} -$$

$$a_{12} = -\alpha_1 u(1-m); a_{13} = \frac{ru^2(k+k_0) - ru^3 - rk k_0 u}{(a_1 + w_0 - w)^2 k^2 k_0}; a_{21} = \frac{a_2 v(1-m)}{(a_2 + w_0 - w)} - av(1-m); a_{22} = \frac{a_2 u(1-m)}{(a_2 + w_0 - w)} - \delta_2 - au(1-m); a_{23} = \frac{a_2 u(1-m)v}{(a_2 + w_0 - w)^2};$$

$$a_{31} = d - \gamma_1 w; a_{32} = -\gamma_2 w; a_{33} = -(s + \gamma + \gamma_1 u + \gamma_2 v).$$

Keeping this in mind, we take a look at the DOPZ system around each equilibrium.

1. The Jacobian matrix at the DOEP $F_1 = (0, 0, \hat{w})$ is given as:

$$J(F_1) = \begin{bmatrix} -\frac{r}{(a_1 + w_0 - \hat{w})} - \delta_1 & 0 & 0 \\ 0 & -\delta_2 & 0 \\ d - \gamma_1 \hat{w} & -\gamma_2 \hat{w} & -s - \gamma \end{bmatrix} \quad (5)$$

Then, $J(F_1)$ has the eigenvalues $\lambda_{11} = \frac{-r}{(a_1 + w_0 - \hat{w})} - \delta_1 < 0$, $\lambda_{12} = -\delta_2 < 0$, and $\lambda_{13} = -s - \gamma < 0$, which means F_1 is a locally asymptotically stable point.

2. The Jacobian matrix at the ZFEP $F_2 = (\bar{u}, 0, \bar{w})$ is given as:

$$J(F_2) = \begin{bmatrix} a_{11}^{[2]} & a_{12}^{[2]} & a_{13}^{[2]} \\ a_{21}^{[2]} & a_{22}^{[2]} & a_{23}^{[2]} \\ a_{31}^{[2]} & a_{32}^{[2]} & a_{33}^{[2]} \end{bmatrix}, \quad (6)$$

where $a_{11}^{[2]} = \frac{2\bar{r}\bar{u}(k+k_0)-3\bar{r}\bar{u}^2-rk\bar{k}_0}{(a_1+w_0-\bar{w})k\bar{k}_0}$; $a_{12}^{[2]} = -\alpha_1\bar{u}(1-m)$; $a_{13}^{[2]} = \frac{\bar{r}\bar{u}^2(k+k_0)-\bar{r}\bar{u}^3-rk\bar{k}_0\bar{u}}{(a_1+w_0-\bar{w})^2k^2\bar{k}_0^2}$; $a_{21}^{[2]} = 0$; $a_{22}^{[2]} = \frac{\alpha_2\bar{u}(1-m)}{(a_2+w_0-\bar{w})} - \delta_2 - a\bar{u}(1-m)$; $a_{23}^{[2]} = 0$; $a_{31}^{[2]} = d - \gamma_1\bar{w}$; $a_{32}^{[2]} = -\gamma_2\bar{w}$; $a_{33}^{[2]} = -s - \gamma - \gamma_1\bar{u}$.

Then, the characteristic equation of $J(F_2)$ is given by:

$$\left(\frac{\alpha_2\bar{u}(1-m)}{(a_2+w_0-\bar{w})} - \delta_2 - a\bar{u}(1-m) - \lambda \right) [\lambda^2 - \text{Tr}(J(F_2))\lambda + \text{Det}(J(F_2))].$$

The eigenvalues of the above equation can be written as follows.

$$\lambda_{21} = \frac{\alpha_2\bar{u}(1-m)}{(a_2+w_0-\bar{w})} - \delta_2 - a\bar{u}(1-m),$$

$$\text{Tr}(J(F_2)) = \frac{2\bar{r}\bar{u}(k+k_0)-3\bar{r}\bar{u}^2-rk\bar{k}_0}{(a_1+w_0-\bar{w})k\bar{k}_0} - (s+\gamma+\gamma_1\bar{u})(a_1+w_0-\bar{w})k\bar{k}_0,$$

$$\text{Det}(J(F_2)) = \frac{2\bar{r}\bar{u}(k+k_0)-3\bar{r}\bar{u}^2-rk\bar{k}_0}{(a_1+w_0-\bar{w})k\bar{k}_0} \left[-s-\gamma-\gamma_1\bar{u} \right] - \left[\frac{\bar{r}\bar{u}^2(k+k_0)-3\bar{r}\bar{u}^3-rk\bar{k}_0\bar{u}}{(a_1+w_0-\bar{w})^2k^2\bar{k}_0^2} \right] [d - \gamma_1\bar{w}].$$

Clearly, F_2 exhibits local asymptotic stability if and only if the following conditions are fulfilled:

$$\left. \begin{aligned} \delta_2 + a\bar{u}(1-m) &> \frac{\alpha_2\bar{u}(1-m)}{(a_2+w_0-\bar{w})}, \\ 2\bar{r}\bar{u}(k+k_0) &< 3\bar{r}\bar{u}^3 + rk\bar{k}_0 + (s+\gamma+\gamma_1\bar{u})(a_1+w_0-\bar{w})k\bar{k}_0, \\ \text{Det}(J(F_2)) &> 0. \end{aligned} \right\} \quad (7)$$

3. The Jacobian matrix at the CEP $F_3 = (u^*, v^*, w^*)$ is given as:

$$J(F_3) = \begin{bmatrix} a_{11}^{[3]} & a_{12}^{[3]} & a_{13}^{[3]} \\ a_{21}^{[3]} & a_{22}^{[3]} & a_{23}^{[3]} \\ a_{31}^{[3]} & a_{32}^{[3]} & a_{33}^{[3]} \end{bmatrix} \quad (8)$$

where, $a_{11}^{[3]} = \frac{2ru^*(k+k_0)-3ru^2-rk\bar{k}_0}{(a_1+w_0-w^*)k\bar{k}_0} - \delta_1 - \alpha_1v^*(1-m)$; $a_{12}^{[3]} = -\alpha_1u^*(1-m)$; $a_{13}^{[3]} = \frac{ru^{*2}(k+k_0)-ru^{*3}-rk\bar{k}_0u^*}{(a_1+w_0-w^*)^2k^2\bar{k}_0^2}$; $a_{21}^{[3]} = \frac{\alpha_2v^*(1-m)}{(a_2+w_0-w^*)} - av^*(1-m)$; $a_{22}^{[3]} = 0$; $a_{23}^{[3]} = \frac{\alpha_2u^*(1-m)v^*}{(a_2+w_0-w^*)^2}$; $a_{31}^{[3]} = d - \gamma_1w^*$; $a_{32}^{[3]} = -\gamma_2w^*$; $a_{33}^{[3]} = -s - \gamma - \gamma_1u^* - \gamma_2v^*$.

Therefore, the characteristic equation of $J(F_3)$ is represented as:

$$\lambda^3 + A_1\lambda^2 + A_2\lambda + A_3 = 0, \quad (9)$$

where,

$$A_1 = -(a_{11}^{[3]} + a_{33}^{[3]}),$$

$$A_2 = -(a_{13}^{[3]}a_{31}^{[3]} + a_{23}^{[3]}a_{32}^{[3]} + a_{12}^{[3]}a_{21}^{[3]} - a_{11}^{[3]}a_{33}^{[3]}),$$

$$A_3 = a_{11}^{[3]}a_{23}^{[3]}a_{32}^{[3]} + a_{12}^{[3]}a_{21}^{[3]}a_{33}^{[3]} - a_{13}^{[3]}a_{21}^{[3]}a_{32}^{[3]} - a_{12}^{[3]}a_{23}^{[3]}a_{31}^{[3]},$$

$$\Delta = A_1A_2 - A_3 = (a_{11}^{[3]} + a_{33}^{[3]})(a_{13}^{[3]}a_{31}^{[3]} - a_{11}^{[3]}a_{33}^{[3]}) + a_{11}^{[3]}a_{12}^{[3]}a_{21}^{[3]} + a_{23}^{[3]}a_{32}^{[3]}a_{33}^{[3]} + a_{12}^{[3]}a_{23}^{[3]}a_{31}^{[3]} + a_{13}^{[3]}a_{21}^{[3]}a_{32}^{[3]}.$$

Now, from the Routh-Hurwitz criteria [32], F_3 is a LAS point, under the condition that $A_1 > 0$, $A_3 > 0$ and $\Delta > 0$.

In the following theorem, adequate conditions for the global stability of the CEP, which is given by $F_3 = (u^*, v^*, w^*)$ are identified by the Lyapunov method [33].

Theorem 3. Assume that

$$\left. \begin{aligned} [d + w^*]^2 &\leq \frac{4c_1r}{k\bar{k}_0} [(u + u^*) - (k + k_0)][s + \gamma + \gamma_1u + \gamma_2v] \\ w^*(v - v^*)(w - w^*) &< \left[\sqrt{\frac{c_1r}{k\bar{k}_0} [(u + u^*) - (k + k_0)] + \sqrt{s + \gamma + \gamma_1u + \gamma_2v}} \right]^2 \\ \alpha_2 &> a \end{aligned} \right\} \quad (10)$$

then CEP is globally asymptotically stable in R_+^3 .

Proof: Define $G_3 = c_1(u - u^* - u^* \ln \frac{u}{u^*}) + c_2(v - v^* - v^* \ln \frac{v}{v^*}) + c_3(\frac{w-w^*}{2})^2$, where c_1 , c_2 and c_3 are positive constants to be specified and $G_3(u, v, w)$ is a positive definite function of CEP. Thus,

$$\frac{dG_3}{dt} \leq c_1(u - u^*) \left[-\frac{ru^2}{k\bar{k}_0} + \frac{r(k+k_0)u}{k\bar{k}_0} - r + \frac{ru^2}{k\bar{k}_0} - \frac{r(k+k_0)u^*}{k\bar{k}_0} + r - \alpha_1(1-m)(v - v^*) \right] + c_2(v - v^*)[(\alpha_2 - a)(1-m)(u - u^*)] + c_3(w - w^*)[-(s + \gamma)(w - w^*) + d(u - u^*) - \gamma_1u(w - w^*) + w^*(u - u^*) - \gamma_2v(w - w^*) + w^*(v - v^*)].$$

Therefore,

$$\frac{dG_3}{dt} \leq -\frac{c_1r(u-u^*)^2}{k\bar{k}_0} [(u + u^*) - (k + k_0)] - (1-m)(u - u^*)(v - v^*)[c_1\alpha_1 - c_2\alpha_2 + c_2a] - c_3(w - w^*)^2[(s + \gamma) + \gamma_1u + \gamma_2v] + c_3(u - u^*)(w - w^*)[d + w^*] + c_3w^*(v - v^*)(w - w^*).$$

By choosing the constants as: $c_2 = c_3 = 1$ and $c_1 = \frac{(\alpha_2 - a)}{\alpha_1}$, the following is obtained,

$$\frac{dG_3}{dt} \leq -\frac{c_1r}{k\bar{k}_0} [(u + u^*) - (k + k_0)](u - u^*)^2 + [d + w^*](u - u^*)(w - w^*) - [(s + \gamma) + \gamma_1u + \gamma_2v](w - w^*)^2 + w^*(v - v^*)(w - w^*).$$

After some algebraic computation, we obtain

$$\frac{dG_3}{dt} \leq - \left[\sqrt{\frac{c_1r}{k\bar{k}_0} [(u + u^*) - (k + k_0)]} (u + u^*) + \sqrt{s + \gamma + \gamma_1u + \gamma_2v} (w - w^*) \right]^2 + w^*(v - v^*)(w - w^*).$$

Then, $\frac{dG_3}{dt} < 0$ under condition (10). Hence, G_3 is a Lyapunov function. Therefore, CEP is globally asymptotically stable in R_+^3 if u , v and w are controlled as in condition (10).

3.4. Local bifurcation

Bifurcation theory looks at how the structure of a group of curves, like the solutions to a set of differential equations, can change over time. A bifurcation happens when a small, smooth change in the values of a system's parameters causes a big change in the way it acts. It is most often used in mathematics to study systems that change over time. Local bifurcations happen when parameters cross critical thresholds and cause changes in the local stability of equilibria. In this section, it is checked to see if there is a chance of local bifurcation. See Refs. [27,34] for a comprehensive treatment. To this end, we rewrite the DOPZ model as follows:

$$\frac{dU}{dt} = F(U), \text{ with } U = \begin{pmatrix} u \\ v \\ w \end{pmatrix}, \text{ and } F = \begin{pmatrix} f_1(u, v, w) \\ f_2(u, v, w) \\ f_3(u, v, w) \end{pmatrix}.$$

For a nonzero vector $Z = (z_1, z_2, z_3)^T$ we set

$$D^2F(z, z) = \begin{bmatrix} c_{11} \\ c_{21} \\ c_{31} \end{bmatrix}, \quad (11)$$

where,

$$c_{11} = \frac{[2r(k+k_0)-6ru]z_1^2}{(a_1+w_0-w)k\bar{k}_0} - 2\alpha_1(1-m)z_1z_2 + \left[\frac{2ru(k+k_0)-3ru^2-rk\bar{k}_0}{(a_1+w_0-w)^2} \right] [z_1z_3 + \frac{z_1z_3}{k^2\bar{k}_0^2}] + \left[\frac{2ru^2(k+k_0)-2ru^3-2rk\bar{k}_0u}{(a_1+w_0-w)^3k^2\bar{k}_0^2} \right],$$

$$c_{21} = \frac{2\alpha_2(1-m)}{(a_2+w_0-w)} \left[z_1z_2 - \frac{uvz_2^2}{(a_2+w_0-w)^2} \right] - 2a(1-m)z_1z_2,$$

$$c_{31} = -2\gamma_1z_1z_3 - 2\gamma_2z_2z_3.$$

Theorem 4. For $\alpha_2^* = \frac{[\delta_2 + a\bar{u}(1-m)](a_2+w_0-\bar{w})}{\bar{u}(1-m)}$, the DOPZ model, at F_2 has

- 1) no saddle-node bifurcation.
 - 2) a transcritical bifurcation if
- $$(p^{[2]})^T [D^2F(F_2, \alpha_2^*) (Z^{[2]}, Z^{[2]})] \neq 0 \quad (12)$$

3) a pitchfork bifurcation if condition (12) is violated and the following statement is satisfied

$$(P^{[2]})^T [D^3 F(F_2, \alpha_2^*) (Z^{[2]}, Z^{[2]}, Z^{[2]})] \neq 0, \quad (13)$$

where the notation in (12) and (13) will be introduced during the proof.

Proof: - At $\alpha_2^* = \frac{(\delta_2 + a\bar{u}(1-m))(a_2 + w_0 - \bar{w})}{\bar{u}(1-m)}$, $J(F_2)$ has a zero eigenvalue $\lambda_{21} = 0$.

0. Therefore, $J(F_2)$ at α_2^* becomes

$$J^*(F_2) = \begin{bmatrix} \frac{2r\bar{u}(k+k_0) - 3r\bar{u}^2 - rkk_0}{(a_1 + w_0 - \bar{w})kk_0} - \delta_1 & -\alpha_1 k & \frac{r\bar{u}^2(k+k_0) - r\bar{u}^3 - rkk_0\bar{u}}{T_2^2 k^2 k_0^2} \\ 0 & 0 & 0 \\ d - \gamma_1 \bar{w} & -\gamma_2 \bar{w} & -s - \gamma - \gamma_1 \bar{u} \end{bmatrix}.$$

Now, let $Z^{[2]} = (z_1^{[2]}, z_2^{[2]}, z_3^{[2]})^T$ be an eigenvector corresponding to $\lambda_{21} = 0$.

0. Thus $(J^*(F_2) - \lambda_{21}I)Z^{[2]} = 0$, which gives:

$$z_1^{[2]} = \frac{[\alpha_1 \bar{u}(1-m)e_1 e_3^2 + e_2 \gamma_2 \bar{w}]z_3^{[2]}}{[(e_4 - \gamma_1 e_3)e_1 e_3 + e_2(d - \gamma_1 \bar{w})]kk_0}, z_3^{[2]} = \frac{(d - \gamma_1 \bar{w})z_1^{[2]} - \gamma_2 \bar{w}z_2^{[2]}}{s + \gamma + \gamma_1 \bar{u}} \text{ and } z_2^{[2]} \text{ represents any nonzero real number, where } (e_4 - \gamma_1 e_3)e_1 e_3 + e_2(d - \gamma_1 \bar{w}) \neq 0 \text{ and } e_1 = s + \gamma + \gamma_1 \bar{u}; e_2 = r\bar{u}^2(k+k_0) - r\bar{u}^3 - rkk_0\bar{u}; e_3 = (a_1 + w_0 - \bar{w})kk_0; e_4 = 2r\bar{u}(k+k_0) - 3r\bar{u}^2 - rkk_0. \text{ That means}$$

$$Z^{[2]} = \left(\frac{[\alpha_1 \bar{u}(1-m)e_1 e_3^2 + e_2 \gamma_2 \bar{w}]z_3^{[2]}}{[(e_4 - \gamma_1 e_3)e_1 e_3 + e_2(d - \gamma_1 \bar{w})]kk_0}, z_2^{[2]}, \frac{(d - \gamma_1 \bar{w})z_1^{[2]} - \gamma_2 \bar{w}z_2^{[2]}}{s + \gamma + \gamma_1 \bar{u}} \right)^T.$$

Let $P^{[2]} = (p_1^{[2]}, p_2^{[2]}, p_3^{[2]})^T$ be an eigenvector associated with $\lambda_{21} = 0$ of the matrix J_2^{*T} . Then $(J_2^{*T} - \lambda_{21}I)P^{[2]} = 0$. By solving this equation for $P^{[2]}$, $P^{[2]} = (p_1^{[2]}, p_2^{[2]}, \frac{r\bar{u}^2(k+k_0) - r\bar{u}^3 - rkk_0\bar{u}}{(a_1 + w_0 - \bar{w})^2 k^2 k_0^2 (s + \gamma + \gamma_1 \bar{u})})^T$ is obtained, where $p_1^{[2]}$ and $p_2^{[2]}$ is any nonzero real number.

Then, the following is taken into account to check if saddle-node bifurcation meets the criteria of Sotomayor's theorem [35]:

$$\frac{\partial F}{\partial \alpha_2} = F_{\alpha_2}(F_2, \alpha_2) = \left(\frac{\partial f_1}{\partial \alpha_2}, \frac{\partial f_2}{\partial \alpha_2}, \frac{\partial f_3}{\partial \alpha_2} \right)^T = \left(0, \frac{uv(1-m)}{(a_2 + w_0 - \bar{w})}, 0 \right)^T.$$

So, $F_{\alpha_2}(F_2, \alpha_2^*) = (0, 0, 0)^T$.

Therefore, the first criterion for transcritical bifurcation or pitchfork bifurcation holds, whilst saddle-node bifurcation cannot arise. Subsequently,

$$DF_{\alpha_2}(F_2, \alpha_2^*) = \begin{bmatrix} 0 & 0 & 0 \\ 0 & \frac{\bar{u}(1-m)}{(a_2 + w_0 - \bar{w})} & 0 \\ 0 & 0 & 0 \end{bmatrix}.$$

where, $DF_{\alpha_2}(S, \alpha_2)$ represents the derivative of $F_{\alpha_2}(S, \alpha_2)$ with respect to $S = (u, v, w)^T$. Furthermore,

$$DF_{\alpha_2}(F_2, \alpha_2^*)Z^{[2]} = \begin{bmatrix} 0 & 0 & 0 \\ 0 & \frac{\bar{u}(1-m)}{(a_2 + w_0 - \bar{w})} & 0 \\ 0 & 0 & 0 \end{bmatrix} \begin{bmatrix} z_1^{[2]} \\ z_2^{[2]} \\ z_3^{[2]} \end{bmatrix}.$$

$$(P^{[2]})^T DF_{\alpha_2}(F_2, \alpha_2^*)Z^{[2]} = (p_1^{[2]}, p_2^{[2]}, p_3^{[2]}) \left(0, \frac{\bar{u}(1-m)z_2^{[2]}}{(a_2 + w_0 - \bar{w})}, 0 \right)^T =$$

$$\frac{\bar{u}(1-m)z_2^{[2]}p_2^{[2]}}{(a_2 + w_0 - \bar{w})} \neq 0.$$

Therefore, the second condition for transcritical or pitchfork bifurcation holds.

Next, we assume that condition (12) holds, i.e.

$$(P^{[2]})^T [D^2 F(F_2, \alpha_2^*) (Z^{[2]}, Z^{[2]})] \neq 0.$$

This implies that the necessary conditions for a transcritical bifurcation are met.

Finally, if condition (12) is not satisfied, then the first, second and third conditions of pitchfork bifurcation are satisfied according to Sotomayor's theorem. Further, we have

$$D^3 F(Z, Z, Z) = \begin{bmatrix} x_{11} \\ x_{21} \\ x_{31} \end{bmatrix},$$

where,

$$x_{11} = - \frac{6r\bar{u}^2}{(a_1 + w_0 - \bar{w})kk_0} + \left[\frac{2r(k+k_0) - 6r\bar{u}}{(a_1 + w_0 - \bar{w})^2} \right] \left[2z_1^2 z_3 + \frac{z_1^2 z_3}{k^2 k_0^2} \right] +$$

$$\left[\frac{4ru(k+k_0) - 6ru^2 - 2rkk_0}{(a_1 + w_0 - \bar{w})^3} \right] \left[z_1 z_3^2 + \frac{2z_1 z_3^2}{k^2 k_0^2} \right] + \frac{6ru(u(k+k_0) - u^2 - kk_0)z_3^2}{(a_1 + w_0 - \bar{w})^4 k^2 k_0^2};$$

$$x_{21} = \frac{2\alpha_2(1-m)z_3}{(a_2 + w_0 - \bar{w})^2} \left[z_1 z_2 - \frac{vz_1 z_3}{(a_2 + w_0 - \bar{w})} - \frac{uz_2 z_3}{(a_2 + w_0 - \bar{w})} - \frac{3uvz_3^2}{(a_2 + w_0 - \bar{w})^2} \right]; x_{31} = 0.$$

Hence,

$$(P^{[2]})^T [D^3 F(F_2, \alpha_2^*) (Z^{[2]}, Z^{[2]}, Z^{[2]})] = (p_1^{[2]}, p_2^{[2]}, p_3^{[2]}) \left(- \frac{6r[z_1^{[2]}]^3}{(a_1 + w_0 - \bar{w})kk_0} + \left[\frac{2r(k+k_0) - 6r\bar{u}}{(a_1 + w_0 - \bar{w})^2} \right] \left[2[z_1^{[2]}]^2 z_3 + \frac{[z_1^{[2]}]^2 z_3}{k^2 k_0^2} \right] + \left[\frac{4r\bar{u}(k+k_0) - 6r\bar{u}^2 - 2rkk_0}{(a_1 + w_0 - \bar{w})^3} \right] \left[z_1^{[2]} [z_3^{[2]}]^2 + \frac{2z_1^{[2]} [z_3^{[2]}]^2}{k^2 k_0^2} \right] + \frac{6r\bar{u}\bar{u}(k+k_0) - \bar{u}^2 - kk_0}{(a_1 + w_0 - \bar{w})^4 k^2 k_0^2} \left[z_1^{[2]} z_2^{[2]} z_3^{[2]} - \frac{z_2^{[2]} [z_3^{[2]}]^2}{k^2 k_0^2} \right], 0 \right)^T.$$

$$= - \frac{6r[z_1^{[2]}]^3 p_1^{[2]}}{(a_1 + w_0 - \bar{w})kk_0} + \left[\frac{2r(k+k_0) - 6r\bar{u}}{(a_1 + w_0 - \bar{w})^2} \right] \left[2[z_1^{[2]}]^2 z_3 + \frac{[z_1^{[2]}]^2 z_3}{k^2 k_0^2} \right] p_1^{[2]} + \left[\frac{4r\bar{u}(k+k_0) - 6r\bar{u}^2 - 2rkk_0}{(a_1 + w_0 - \bar{w})^3} \right] \left[z_1^{[2]} [z_3^{[2]}]^2 + \frac{2z_1^{[2]} [z_3^{[2]}]^2}{k^2 k_0^2} \right] p_1^{[2]} + \frac{6r\bar{u}\bar{u}(k+k_0) - \bar{u}^2 - kk_0}{(a_1 + w_0 - \bar{w})^4 k^2 k_0^2} [z_1^{[2]} z_2^{[2]} z_3^{[2]} - \frac{z_2^{[2]} [z_3^{[2]}]^2}{k^2 k_0^2}] p_2^{[2]}.$$

This means if condition (13) is satisfied, then the DOPZ model has a pitchfork bifurcation at F_2 with the parameter α_2^* .

Theorem 5. For $\gamma_2^* = \frac{a_{11}^{[3]}(a_{13}^{[3]}a_{31}^{[3]} + a_{12}^{[3]}a_{21}^{[3]} + a_{11}^{[3]}a_{33}^{[3]} - [a_{31}^{[3]}]^2) + a_{13}^{[3]}(a_{31}^{[3]}a_{33}^{[3]} + a_{12}^{[3]}a_{23}^{[3]} - [a_{23}^{[3]}]^2) + a_{12}^{[3]}(a_{23}^{[3]}a_{33}^{[3]} + a_{11}^{[3]}a_{33}^{[3]} - [a_{33}^{[3]}]^2)}{[a_{23}^{[3]}a_{33}^{[3]} + a_{12}^{[3]}a_{31}^{[3]}]w^*}$, where the formulas of $a_{ij}^{[3]} = d_{ij}$ are given in the following proof, the DOPZ model at CEP has a saddle-node bifurcation if

$$D^2 F(F_3, \gamma_1^*) (Z^{[3]}, Z^{[3]}) \neq 0 \quad (14)$$

Proof: - According to $J(F_3)$, given by (8), the DOPZ model at CEP has a zero eigenvalue, say $\lambda_{31} = 0$, at $\gamma_2^* = \frac{a_{11}^{[3]}(a_{13}^{[3]}a_{31}^{[3]} + a_{12}^{[3]}a_{21}^{[3]} + a_{11}^{[3]}a_{33}^{[3]} - [a_{31}^{[3]}]^2) + a_{13}^{[3]}(a_{31}^{[3]}a_{33}^{[3]} + a_{12}^{[3]}a_{23}^{[3]} - [a_{23}^{[3]}]^2) + a_{12}^{[3]}(a_{23}^{[3]}a_{33}^{[3]} + a_{11}^{[3]}a_{33}^{[3]} - [a_{33}^{[3]}]^2)}{[a_{23}^{[3]}a_{33}^{[3]} + a_{12}^{[3]}a_{31}^{[3]}]w^*}$, where $(a_{32}^{[3]}a_{33}^{[3]} + a_{12}^{[3]}a_{31}^{[3]}) \neq 0$ and the Jacobian matrix $J^*(F_3) = J(F_3, \gamma_2^*)$, becomes:

$$J^*(F_3) = \begin{bmatrix} d_{11} & d_{12} & d_{13} \\ d_{21} & d_{22} & d_{23} \\ d_{31} & d_{32} & d_{33} \end{bmatrix}.$$

$$d_{11} = \frac{2ru^*(k+k_0) - 3ru^{*2} - rkk_0}{(a_1 + w_0 - w^*)kk_0} - \alpha_1 v(1-m) - \delta_1;$$

$$d_{12} = -\alpha_1 u^*(1-m); d_{13} = \frac{ru^{*2}(k+k_0) - ru^{*3} - rkk_0 u^*}{(a_1 + w_0 - w^*)^2 k^2 k_0^2}; d_{21} = \frac{\alpha_2 v^*(1-m)}{(a_2 + w_0 - w^*)} - av^*(1-m); d_{22} = 0; d_{23} = \frac{\alpha_2 u^*(1-m)v^*}{(a_2 + w_0 - w^*)^2 k^2 k_0^2}; d_{31} = d - \gamma_1 w^*; d_{32} = -\gamma_2^* w^*;$$

$d_{33} = -s - \gamma - \gamma_1 u^* - \gamma_2^* v^*$. Now, let $Z^{[3]} = (z_1^{[3]}, z_2^{[3]}, z_3^{[3]})^T$ be an eigenvector corresponding to $\lambda_{31} = 0$. Thus $(J^*(F_3) - \lambda_{31}I)Z^{[3]} = 0$, which implies: $z_1^{[3]} = \frac{-d_{23}z_3^{[3]}}{d_{21}}$, $z_2^{[3]} = \frac{(d_{31}d_{23} - d_{21}d_{33})z_3^{[3]}}{d_{21}d_{23}}$, where $d_{21} \neq 0$ and $z_3^{[3]}$ represents any nonzero real number. That means $Z^{[3]} = (z_1^{[3]}, z_2^{[3]}, z_3^{[3]})^T$.

Let $P^{[3]} = (p_1^{[3]}, p_2^{[3]}, p_3^{[3]})^T$ be an eigenvector associated with $\lambda_{31} = 0$ of the matrix $J^*(F_3)$. Then $(J_3^{*T} - \lambda_{31}I)P^{[3]} = 0$. By solving this equation for $P^{[3]}$, $P^{[3]} = \left(\frac{-d_{32}p_3^{[3]}}{d_{12}}, \left[\frac{d_{13}d_{32} - d_{12}d_{33}}{d_{12}d_{23}} \right] p_3^{[3]}, p_3^{[3]} \right)^T$ is obtained, where $P_3^{[3]}$ is any nonzero real number.

Now, the following are quantified to ensure that Sotomayor's theorem for saddle-node bifurcation holds:

$$\frac{\partial F}{\partial \gamma_2} = \left(\frac{\partial f_1}{\partial \gamma_2}, \frac{\partial f_2}{\partial \gamma_2}, \frac{\partial f_3}{\partial \gamma_2} \right)^T = (0, 0, -vw)^T.$$

So, $F_{\gamma_2} = (F_3, \gamma_2^*) = (0, 0, -v^*w^*)^T$ and hence $(P^{[3]})^T F_{\gamma_2}(F_3, \gamma_2^*) = -v^*w^*p_3^{[3]} \neq 0$.

Hence, the first requirement for saddle-node bifurcation is satisfied, but transcritical or pitchfork bifurcation is not possible. Subsequently,

$$D^2 F(F_3, \gamma_1^*) (Z^{[3]}, Z^{[3]}) = \left(\frac{2r(k+k_0) - 6ru^*}{(a_1 + w_0 - w^*)^2} - 2\alpha_1(1-m)z_1^{[3]}z_2 + \left[\frac{2ru^*(k+k_0) - 3ru^{*2} - rkk_0}{(a_1 + w_0 - w^*)^2} \right] \left[z_1^{[3]} z_3^{[3]} + \frac{z_1^{[3]} z_3^{[3]}}{k^2 k_0^2} \right] + 2ru^*[u^*(k+k_0) - u^{*2} - kk_0] \frac{[z_3^{[3]}]^2}{k^2 k_0^2} \right)^T.$$

$$+ \frac{6r\bar{u}\bar{u}(k+k_0) - \bar{u}^2 - kk_0}{(a_1 + w_0 - \bar{w})^4 k^2 k_0^2} \left[z_1^{[3]} z_2^{[3]} z_3^{[3]} - \frac{u^* v^* [z_3^{[3]}]^2}{(a_2 + w_0 - w^*)^2} \right] - 2a(1-m)z_1^{[3]}z_2^{[3]} - 2\gamma_1 z_1^{[3]}z_3^{[3]} - 2\gamma_2^* z_2^{[3]}z_3^{[3]} \right)^T.$$

Hence, condition (14) guarantees that the second condition of saddle-node bifurcation is satisfied. Therefore, the DOPZ model has saddle-node

bifurcation at CEP with the parameter γ_2^* .

From Theorem 6, the Bendixson–Dulac criterion [13] is used to find the conditions that guarantee the DOPZ model has no periodic behaviour (Hopf bifurcation) in the positive quadrant of the uw -plane.

Theorem 6. The DOPZ System has no periodic solution in $R_{+(u,w)}^2$, if one of the following conditions is true for all (u, w) in $R_{+(u,w)}^2$:

$$\frac{r(k+k_0)}{(a_1+w_0-w)kk_0w} < \frac{2ur}{(a_1+w_0-w)kk_0w} + \frac{sw_0}{uw^2} + \frac{d}{w^2}, \frac{r(k+k_0)}{(a_1+w_0-w)kk_0w} > \frac{2ur}{(a_1+w_0-w)kk_0w} + \frac{sw_0}{uw^2} + \frac{d}{w^2} \quad (15)$$

Proof: For any initial value (u, w) in $R_{+(u,w)}^2$, let $E(u, w) = \frac{1}{uw}$, $e_1(u, w) = u \left[\frac{r}{(a_1+w_0-w)} \left(1 - \frac{u}{k}\right) \left(\frac{u}{k_0} - 1\right) - \delta_1 \right]$ and $e_2(u, w) = s(w_0 - w) + du - \gamma w - \gamma_1 uw$.

Clearly, $E(u, w) > 0$ for all $(u, w) \in R_{+}^2$ and it is a C^1 function in $R_{+(u,w)}^2 = \{(u, w), u > 0, w > 0\}$.

Thus $\Delta(u, w) = \frac{\partial}{\partial u}(Ee_1) + \frac{\partial}{\partial w}(Ee_2) = \frac{-2ru+r(k+k_0)}{(a_1+w_0-w)kk_0w} - \frac{sw_0}{uw^2} - \frac{d}{w^2} < 0$. $\Delta(u, w)$ does not change sign if one of the inequalities given on (15) satisfies and it is not identically zero in $R_{+(u,w)}^2$. Therefore, the DOPZ model has no periodic dynamics in $R_{+(u,w)}^2$.

From Theorem 7, the steady state of ZFEP changes as the parameter γ crosses the threshold value γ^* , which implies that ZFEP may become unstable due to Hopf bifurcation when forced to operate within particular restrictions on its parameters. In the case where we use γ as the bifurcation parameter, the Hopf bifurcation threshold is the positive root of $\text{Tr } J(F_2)|_{\gamma=\gamma^*} = 0$, under the condition $\text{Det } J(F_2)|_{\gamma=\gamma^*} > 0$.

This leads us to the following theorem as a result.

Theorem 7. Assume that the third inequality of condition (7) holds along with the following condition:

$$\gamma^* > 0, \quad (16)$$

where γ^* is defined in the proof of the theorem. Then, the DOPZ model presents a Hopf bifurcation at $\gamma = \gamma^*$ around the ZFEP.

Proof: - The characteristic equation of matrix $J(F_2)$ is

$$\lambda^2 - \text{Tr}(J(F_2))\lambda + \text{Det } J(F_2) = 0 \quad (17)$$

and the prerequisites for the occurrence of the Hopf bifurcation are outlined below.

- a) $[\text{Tr } J(F_2)]|_{\gamma=\gamma^*} = 0$,
- b) $[\text{Det } J(F_2)]|_{\gamma=\gamma^*} > 0$,
- c) $\frac{d}{d\gamma}[\text{Re}(\lambda_{1,2})]|_{\gamma=\gamma^*} \neq 0$ (Transversality condition).

Conditions (a) and (b) have been satisfied at $\gamma^* = \frac{2r\bar{u}(k+k_0)-3r\bar{u}^2+rkk_0}{(a_1+w_0-\bar{w})kk_0} - (s + \gamma_1\bar{u})$. Clearly $\gamma^* > 0$ if Condition 16 holds. At $\gamma = \gamma^*$, the characteristic equation given by (17) is rewritten as $\lambda^2 + \text{Det } J(F_2) = 0$, which has two roots

$$\lambda_{1,2} = \pm i\sqrt{\text{det}J(F_2)} \quad (18)$$

Clearly, at $\gamma = \gamma^*$ there are two purely imaginary eigenvalues λ_1 and λ_2 which are complex conjugates under conditions (7).

Further, we write the general roots of equation (3) in the neighbourhood of γ^* as

$$\lambda_{1,2} = \frac{\text{tr}(J(F_2)) \pm i\sqrt{\text{det}J(F_2)}}{2}, \text{ then}$$

$$\frac{d}{d\gamma}[\text{Re}(\lambda_{1,2})]|_{\gamma=\gamma^*} = \frac{d}{d\gamma} \left[\frac{\text{tr}(J(F_2))}{2} \right]_{\gamma=\gamma^*} = \frac{-1}{2} \neq 0 \quad (19)$$

That means the third condition (c) has been verified, ensuring that when $\gamma = \gamma^*$, a Hopf bifurcation takes place at ZFEP.

In theorem 8, the existence of a Hopf bifurcation around CEP is discussed.

Theorem 8. Under the following assumptions

$$\begin{aligned} A_i > 0, i = 1, 2 \\ a_{12}^{[3]}a_{23}^{[3]} - a_{13}^{[3]}A_1(\gamma_1^*) &\neq 0 \\ \gamma_1^* &> 0. \end{aligned} \quad (20)$$

Here, A_i 's represent the coefficients of the characteristic equation that was mentioned in equation (9) with $\gamma_1 = \gamma_1^*$ and the formula for γ_1^* is given in the below proof. Then, there exists a Hopf bifurcation for CEP at $\gamma_1 = \gamma_1^*$.

Proof: - The value of the bifurcation parameter can be found if we set $A_1(\gamma_1^*)A_2(\gamma_1^*) - A_3(\gamma_1^*) = 0$ in equation (9). This gives:

$$\gamma_1^* = \frac{(d_{11}d_{13}+d_{13}d_{33}+d_{12}d_{23})d+d_{11}(d_{12}d_{21}-d_{11}d_{33}-d_{33}^2)+d_{32}(d_{23}d_{33}+d_{13}d_{21})}{(d_{11}d_{13}+d_{13}d_{33}+d_{12}d_{23})w^*}.$$

Clearly, $\gamma_1^* > 0$ if condition (20) holds. Now, at $\gamma_1 = \gamma_1^*$ Equation (9) can be written as

$$(\lambda + A_1)(\lambda^2 + A_2) = 0.$$

According to condition (18), the above equation has three roots, a negative root $\lambda_1 = -A_1$ and two purely imaginary roots $\lambda_{2,3} = \pm i\sqrt{A_2}$. In a neighbourhood of γ_1^* , the roots have the following forms: $\lambda_1 = -A_1, \lambda_{2,3} = \rho_1(\gamma_1) \pm i\rho_2(\gamma_1)$.

Clearly, $\text{Re}(\lambda_{2,3})|_{\gamma_1=\gamma_1^*} = \rho_1(\gamma_1^*) = 0$ indicates that the first condition for Hopf bifurcation has been met at $\gamma_1 = \gamma_1^*$. Now to confirm the transversality condition, we substitute $\rho_1(\gamma_1) \pm i\rho_2(\gamma_1)$ into equation (9) and then compute its derivative with respect to γ_1^* , $\Theta(\gamma_1^*)\psi(\gamma_1^*) + \Gamma(\gamma_1^*)\varphi(\gamma_1^*) \neq 0$, where the form of $\Theta(\gamma_1^*), \psi(\gamma_1^*), \Gamma(\gamma_1^*)$ and $\varphi(\gamma_1^*)$ are

$$\begin{aligned} \psi(\gamma_1) &= 3\rho_1^2(\gamma_1) + 2A_1(\gamma_1)\rho_1(\gamma_1) + A_2(\gamma_1) - 3\rho_2^2(\gamma_1), \\ \varphi(\gamma_1) &= 6\rho_1(\gamma_1)\rho_2(\gamma_1) + 2A_1(\gamma_1)\rho_2(\gamma_1), \\ \Theta(\gamma_1) &= \rho_1^2(\gamma_1)A_1'(\gamma_1) + A_2'(\gamma_1)\rho_1(\gamma_1) + (\gamma_1 - A_1'(\gamma_1)), \\ \Gamma(\gamma_1) &= 2\rho_1(\gamma_1)\rho_2(\gamma_1)A_1'(\gamma_1) + A_2'(\gamma_1)\rho_2(\gamma_1). \end{aligned}$$

Now at $\gamma_1 = \gamma_1^*$, substitution $\rho_1 = 0$ and $\rho_2 = \sqrt{A_2}$, into equation (9), the following is obtained:

$$\begin{aligned} \psi(\gamma_1^*) &= -2A_2(\gamma_1^*), \\ \varphi(\gamma_1^*) &= 2A_1(\gamma_1^*)\sqrt{A_2(\gamma_1^*)}, \\ \Theta(\gamma_1^*) &= A_3'(\gamma_1^*) - A_1'(\gamma_1^*)A_2(\gamma_1^*), \\ \Gamma(\gamma_1^*) &= A_2'(\gamma_1^*)\sqrt{A_2(\gamma_1^*)}, \end{aligned}$$

where

$$A_1'(\gamma_1^*) = 0, A_2'(\gamma_1^*) = a_{13}^{[3]}w^*, A_3'(\gamma_1^*) = a_{12}^{[3]}a_{23}^{[3]}w^*.$$

Hence, condition (19) gives

$$\Theta(\gamma_1^*)\psi(\gamma_1^*) + \Gamma(\gamma_1^*)\varphi(\gamma_1^*) = -2A_2(\gamma_1^*)w^*[a_{12}^{[3]}a_{23}^{[3]} - a_{13}^{[3]}A_1'(\gamma_1^*)] \neq 0.$$

That means the Hopf bifurcation has occurred at γ_1^* .

From Theorem 9, the stability condition of the stable limit cycle in $R_{(u,v,w)}^3$ is presented using the coefficient of curvature of the limit cycle [36]. For a detailed discussion, we refer to [27].

Theorem 9. The DOPZ System has a stable limit cycle in $R_{(u,v,w)}^3$, if the following conditions are true:

$$\left[\frac{3r(u_1 + u^*) - r(k + k_0)}{8(a_1 + w_0 - u_3 - w^*)kk_0} \right] \alpha_1(1 - m) < \frac{3r}{4(a_1 + w_0 - u_3 - w^*)kk_0} \quad (21)$$

Proof: - We first shift the CEP, $F_3 = (u^*, v^*, w^*)$ to $(0, 0, 0)$ by using the following transformations $u = u_1 + u^*$, $v = u_2 + v^*$, $w = u_3 + w^*$. Then the DOPZ system becomes:

$$\begin{aligned} \frac{du_1}{dt} &= \frac{r(u_1 + u^*)}{(a_1 + w_0 - u_3 - w^*)kk_0} [- (u_1 + u^*)^2 + (u_1 + u^*)(k + k_0) - kk_0] - \alpha_1(u_1 + u^*)(u_2 + v^*)(1 - m) - (u_1 + u^*)\delta_1, \\ \frac{du_2}{dt} &= \frac{\alpha_2(u_1 + u^*)(u_2 + v^*)(1 - m)}{(a_2 + w_0 - u_3 - w^*)} - \delta_2(u_2 + v^*) - a(u_1 + u^*)(u_2 + v^*)(1 - m), \\ \frac{du_3}{dt} &= s[w_0 - (u_3 + w^*)] + d(u_1 + u^*) - \gamma(u_3 + w^*) - \gamma_1(u_1 + u^*)(u_3 + w^*) - \gamma_2(u_2 + v^*)(u_3 + w^*), \end{aligned}$$

where the nonlinear part of the above system is presented in the following matrix is.

$$\bar{U} = \begin{pmatrix} \bar{U}_1 \\ \bar{U}_2 \\ \bar{U}_3 \end{pmatrix} = \begin{pmatrix} \frac{r(u_1 + u^*)}{(a_1 + w_0 - u_3 - w^*)kk_0} [- (u_1 + u^*)^2 + (u_1 + u^*)(k + k_0) - kk_0] - \alpha_1(1 - m)u_1u_2 \\ \frac{\alpha_2(u_1 + u^*)(u_2 + v^*)(1 - m)}{(a_2 + w_0 - u_3 - w^*)} - a(1 - m)u_1u_2 \\ -\gamma_1u_1u_3 - \gamma_2u_2u_3 \end{pmatrix}.$$

We derive the following characteristic quantities from the nonlinear part:

$$\begin{aligned} g_{20}^0 &= \frac{1}{4} \left\{ \frac{\partial^2 \bar{U}_1}{\partial u_1^2} - \frac{\partial^2 \bar{U}_1}{\partial u_1 \partial u_2} + 2 \frac{\partial^2 \bar{U}_2}{\partial u_1 \partial u_2} + i \left(\frac{\partial^2 \bar{U}_2}{\partial u_1^2} - \frac{\partial^2 \bar{U}_2}{\partial u_1 \partial u_2} - 2 \frac{\partial^2 \bar{U}_3}{\partial u_1 \partial u_2} \right) \right\} = \\ &= \frac{1}{2} \left\{ \frac{-3r(u_1 + u^*) + r(k + k_0)}{(a_1 + w_0 - u_3 - w^*)kk_0} + \frac{\alpha_2(1 - m)}{(a_2 + w_0 - u_3 - w^*)} - a(1 - m) + \alpha_1(1 - m)i \right\}, \\ g_{11}^0 &= \frac{1}{4} \left\{ \frac{\partial^2 \bar{U}_1}{\partial u_1^2} + \frac{\partial^2 \bar{U}_1}{\partial u_2^2} + i \left(\frac{\partial^2 \bar{U}_2}{\partial u_1^2} + \frac{\partial^2 \bar{U}_2}{\partial u_2^2} \right) \right\} = \frac{1}{2} \left\{ \frac{-3r(u_1 + u^*) + r(k + k_0)}{(a_1 + w_0 - u_3 - w^*)kk_0} \right\}, \\ g_{110}^0 &= \frac{1}{2} \left\{ \frac{\partial^2 \bar{U}_1}{\partial u_1 \partial u_3} + \frac{\partial^2 \bar{U}_2}{\partial u_2 \partial u_3} + i \left(\frac{\partial^2 \bar{U}_2}{\partial u_1 \partial u_3} - \frac{\partial^2 \bar{U}_1}{\partial u_2 \partial u_3} \right) \right\} = \frac{1}{2} \left\{ \frac{-3r(u_1 + u^*)^2 + 2r(k + k_0)}{(a_1 + w_0 - u_3 - w^*)^2kk_0} - \right. \\ &\quad \left. \frac{r}{(a_1 + w_0 - u_3 - w^*)^2} + \frac{\alpha_2(u_1 + u^*)(1 - m)}{(a_2 + w_0 - u_3 - w^*)^2} + i \left(\frac{\alpha_2(u_2 + v^*)(1 - m)}{(a_2 + w_0 - u_3 - w^*)^2} \right) \right\}, \\ g_{101}^0 &= \frac{1}{2} \left\{ \frac{\partial^2 \bar{U}_1}{\partial u_1 \partial u_3} - \frac{\partial^2 \bar{U}_2}{\partial u_2 \partial u_3} + i \left(\frac{\partial^2 \bar{U}_2}{\partial u_1 \partial u_3} + \frac{\partial^2 \bar{U}_1}{\partial u_2 \partial u_3} \right) \right\} = \frac{1}{2} \left\{ \frac{-3r(u_1 + u^*)^2 + 2r(k + k_0)}{(a_1 + w_0 - u_3 - w^*)^2kk_0} - \right. \\ &\quad \left. \frac{r}{(a_1 + w_0 - u_3 - w^*)^2} - \frac{\alpha_2(u_1 + u^*)(1 - m)}{(a_2 + w_0 - u_3 - w^*)^2} + i \left(\frac{\alpha_2(u_2 + v^*)(1 - m)}{(a_2 + w_0 - u_3 - w^*)^2} \right) \right\}, \\ W_{11}^0 &= -\frac{1}{4\lambda_3(a_1(k^*))} \left(\frac{\partial^2 \bar{U}_3}{\partial u_1^2} + \frac{\partial^2 \bar{U}_3}{\partial u_2^2} \right) = 0, \\ W_{20}^0 &= -\frac{1}{4\lambda_3(a_1(k^*))} \left(\frac{\partial^2 \bar{U}_3}{\partial u_1^2} + \frac{\partial^2 \bar{U}_3}{\partial u_2^2} - 2i \frac{\partial^2 \bar{U}_3}{\partial u_1 \partial u_2} \right) = 0, \\ G_{21}^0 &= \frac{1}{8} \left\{ \frac{\partial^3 \bar{U}_1}{\partial u_1^3} + \frac{\partial^3 \bar{U}_1}{\partial u_1 \partial u_2^2} + \frac{\partial^3 \bar{U}_2}{\partial u_1^2} + \frac{\partial^3 \bar{U}_2}{\partial u_1 \partial u_2} + i \left(\frac{\partial^3 \bar{U}_2}{\partial u_1^3} + \frac{\partial^3 \bar{U}_2}{\partial u_1 \partial u_2^2} - \frac{\partial^3 \bar{U}_1}{\partial u_1^2 \partial u_2} \right) \right\} = \frac{-3r}{4(a_1 + w_0 - u_3 - w^*)kk_0}, \end{aligned}$$

Thus, the coefficient of the curvature of the limit cycle of the DOPZ system

(1) is given by

$$\begin{aligned} \sigma_1^0 &= \text{Re} \left\{ \frac{g_{20}^0 g_{11}^0}{4} i + G_{110}^0 W_{11}^0 + \frac{G_{21}^0 + G_{101}^0 W_{20}^0}{2} \right\}, \\ \sigma_1^0 &= \text{Re} \left\{ \left(\frac{6r^2(u_1 + u^*)^2 + r^2(k + k_0)^2}{8(a_1 + w_0 - u_3 - w^*)^2 k^2 k_0^2} \right) i + \left[\frac{3r(u_1 + u^*) - r(k + k_0)}{8(a_1 + w_0 - u_3 - w^*)kk_0} \right] \alpha_1(1 - m) - \right. \\ &\quad \left. \frac{3r}{4(a_1 + w_0 - u_3 - w^*)kk_0} \right\} = \left[\frac{3r(u_1 + u^*) - r(k + k_0)}{8(a_1 + w_0 - u_3 - w^*)kk_0} \right] \alpha_1(1 - m) - \frac{3r}{4(a_1 + w_0 - u_3 - w^*)kk_0}. \end{aligned}$$

Thus, Condition (21) guarantees that the DOPZ system has a stable limit cycle.

3.5. Numerical simulations

To validate our theoretical conclusions and get insight into the many possible dynamics of the DOPZ model, we conduct a numerical simu-

lation here. In this research, all figures were created in MATLAB 2019b and were constructed and designed similarly to those in Refs. [37–41], and the numerical solution to our system was found using the ode45 solver. Our primary objective is to examine the dynamics of the DOPZ system when the Allee effect is amplified in phytoplankton. For the specified variables:

$$\begin{aligned} r &= 0.445533, k = 4, k_0 = 1, \alpha_1 = 0.4, \alpha_2 = 0.28, \delta_1 = 0.1, \delta_2 = 0.3, m \\ &= 0.36, a_1 = 0.2, a_2 = 0.2, w_0 = 3, a = 0.1, s = 2.85, \gamma_1 \\ &= 0.18, \gamma_2 = 0.2, \gamma = 0.2, d = 1 \end{aligned} \quad (22)$$

and with different initial values, it is observed from Fig. 2 that $F_3 = (1.23, 2.32, 2.61)$ is a globally asymptotically stable point.

To examine the effect of varying one parameter at a time on the behaviour of the DOPZ system, the DOPZ model has been numerically resolved for the data in (22). In light of this, Figs. 3–4 investigate the effect of change in the critical phytoplankton level k_0 (Allee threshold) on the stability behaviour of the DOPZ model. The simulation shows rich dynamics when it is changed. For example, when $k_0 \leq 0.001$, the DOPZ model has no CEP, and the solution settles down to DOEP in the w -axis.

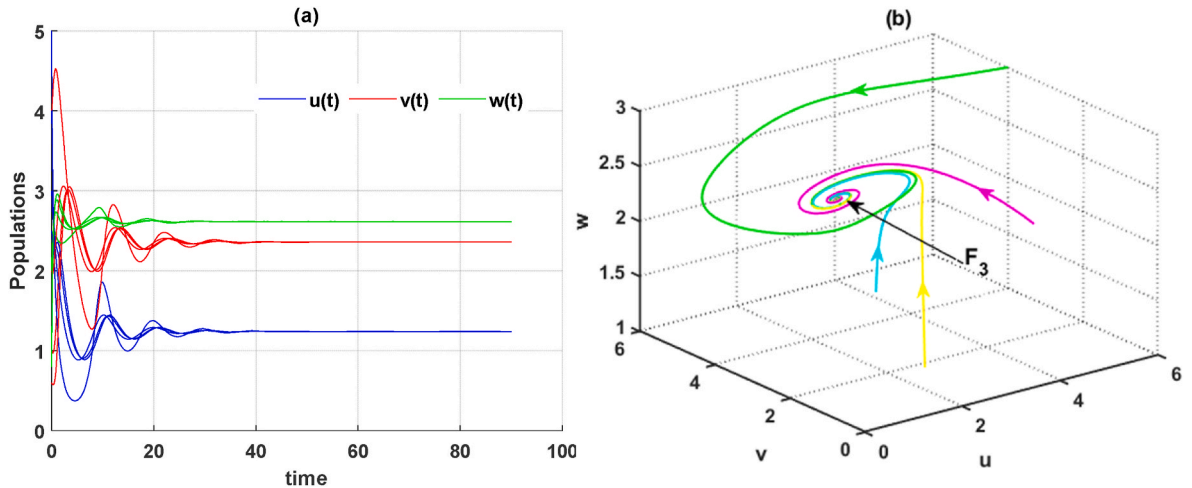


Fig. 2. Phase diagram of the DOPZ model with the data set supplied by (22) and varying initial values.

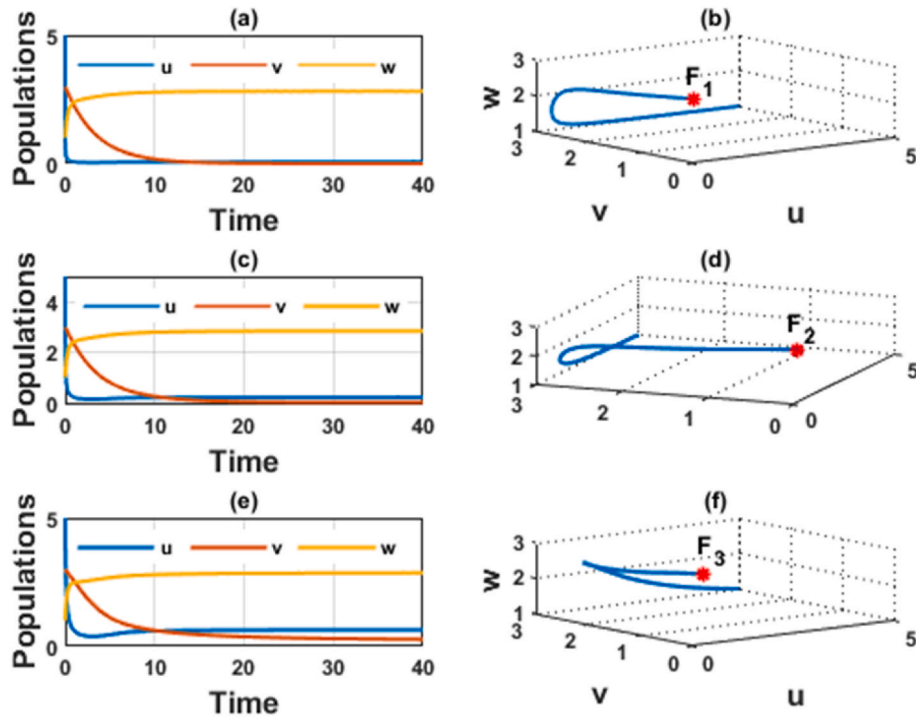


Fig. 3. (a) Time series of the DOPZ system with $k_0 = 0.001$; (b) phase diagram corresponding to (a); (c) time series with $k_0 = 0.01$; (d) phase diagram of (c); (e) time series with $k_0 = 0.1$; (f) phase diagram of (e).

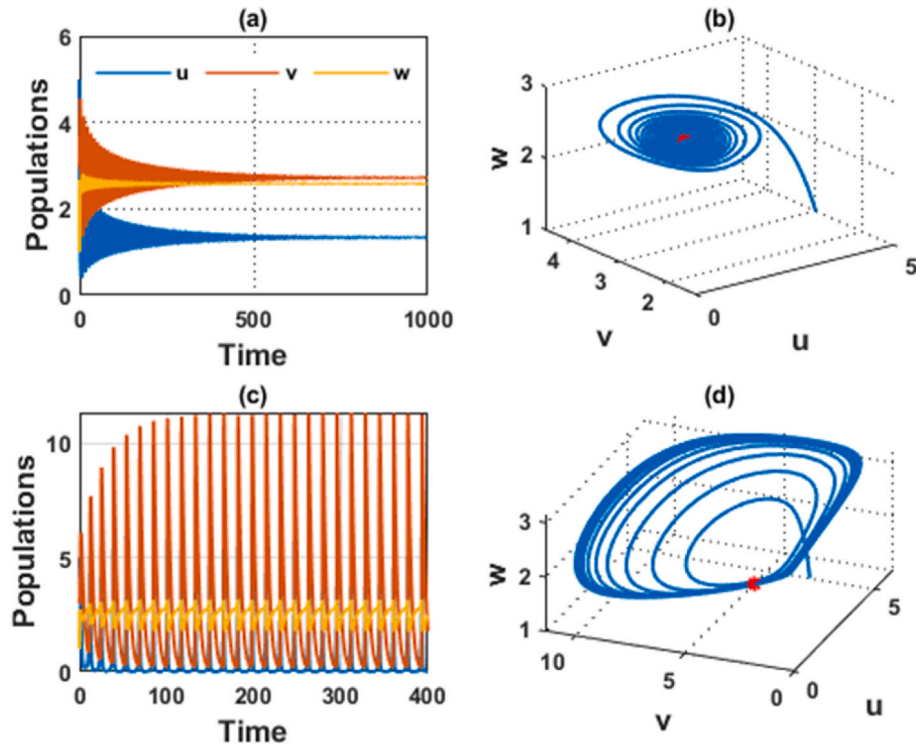


Fig. 4. (a) Time series of the DOPZ system with $k_0 = 2$; (b) phase diagram corresponding to (a); (c) time series with $k_0 = 2.1$; (d) phase diagram of (c).

While for the range $0.001 < k_0 \leq 0.01$, the solution converges asymptotically to ZFEP on uw -plane. For $0.01 < k_0 \leq 2$, the solution converges asymptotically to CEP. On the other hand, for $k_0 \geq 2.1$, the solution shows a periodic attractor behaviour.

Further, Fig. 5 investigates the effect of change in the consumption rate of oxygen by the phytoplankton during the night (γ_1) on the

stability properties of the DOPZ model. It shows for $\gamma_1 \geq 0.78$, the DOPZ model has no CEP, and the solution settles down to ZFEP in the uw -plane. While for the range $0.001 < \gamma_1 < 0.78$, the solution converges asymptotically to CEP in an oscillatory way. On the other hand, for a small $\gamma_1 \leq 0.001$ the solution shows a periodic attractor behaviour. The latter result confirms the one that has been obtained in Theorems 8-9,

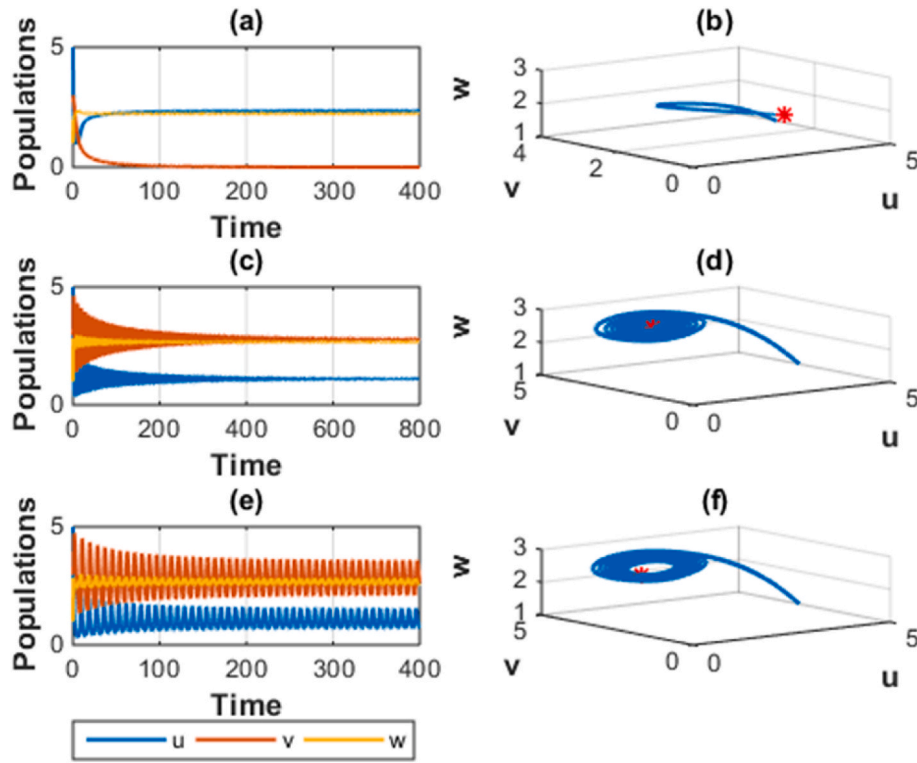


Fig. 5. (a) Time series of the DOPZ system with $\gamma_1 = 0.78$; (b) phase diagram corresponding to (a); (c) time series with $\gamma_1 = 0.01$; (d) phase diagram of (c); (e) time series with $\gamma_1 = 0.001$; (f) phase diagram of (e).

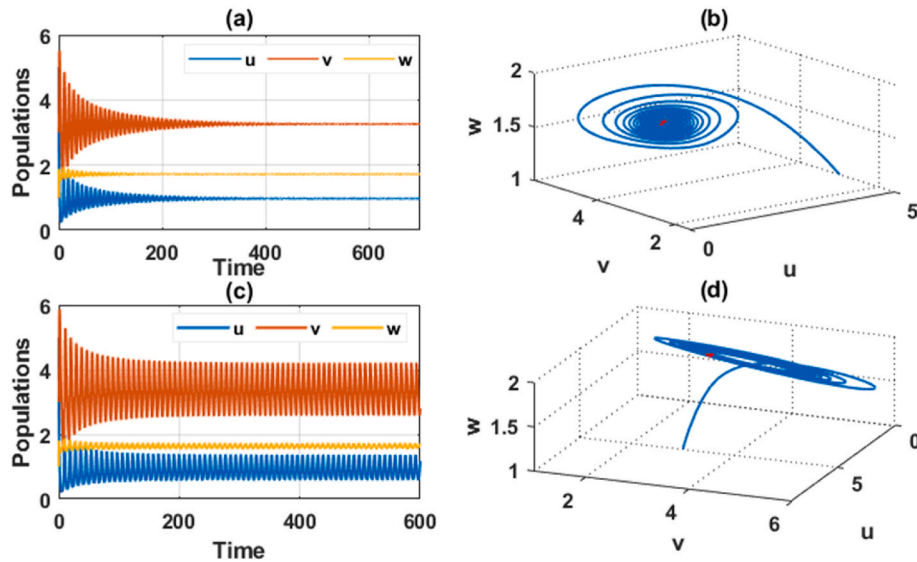


Fig. 6. (a) Time series of the DOPZ system with $w_0 = 2$; (b) phase diagram corresponding to (a); (c) time series with $w_0 = 1.9$; (d) phase diagram of (c).

which establishes the existence of Hopf bifurcation at $\gamma_1^* = 0.001$ and the stability of the obtained limit cycle.

Now the effect of changing the concentration of dissolved oxygen that comes from several sources (w_0) is explored in Fig. 6. The figure shows that the solution settles asymptotically to the CEP, $F_3 = (0.96, 3.26, 1.77)$, for $w_0 > 1.9$. Further, the solution approaches a periodic attractor for $w_0 \leq 1.9$. Accordingly, a decrease in w_0 results in a drop in the DOPZ model's stability, which implies that condition 10 of Theorem 3 is broken and the system's (1) behaviour changes from global stability to periodic behaviour. The system in this instance is getting closer to a stable periodic attractor as a result of this outcome, which satisfies

requirement 21 that is stated in Theorem 9.

Further, Fig. 7 illustrates the impact of varying the phytoplankton's growth rate r , on the behaviour of the DOPZ system. The solution stabilizes at its positive equilibrium point CEP for $r \geq 0.1$. The solution settles down to the dissolved oxygen equilibrium point (F_1) when $r < 0.1$. Consequently, a decrease in r leads to extinction in the plankton populations hence the stability behaviour shifts from the positive equilibrium point (F_3) to the dissolved oxygen equilibrium point (F_1). This result suggests that condition 21 of Theorem 9 is violated, in this case, faces a transcritical bifurcation between F_1 and F_3 .

Next, Fig. 8 depicts the impact of varying the conservation rate from

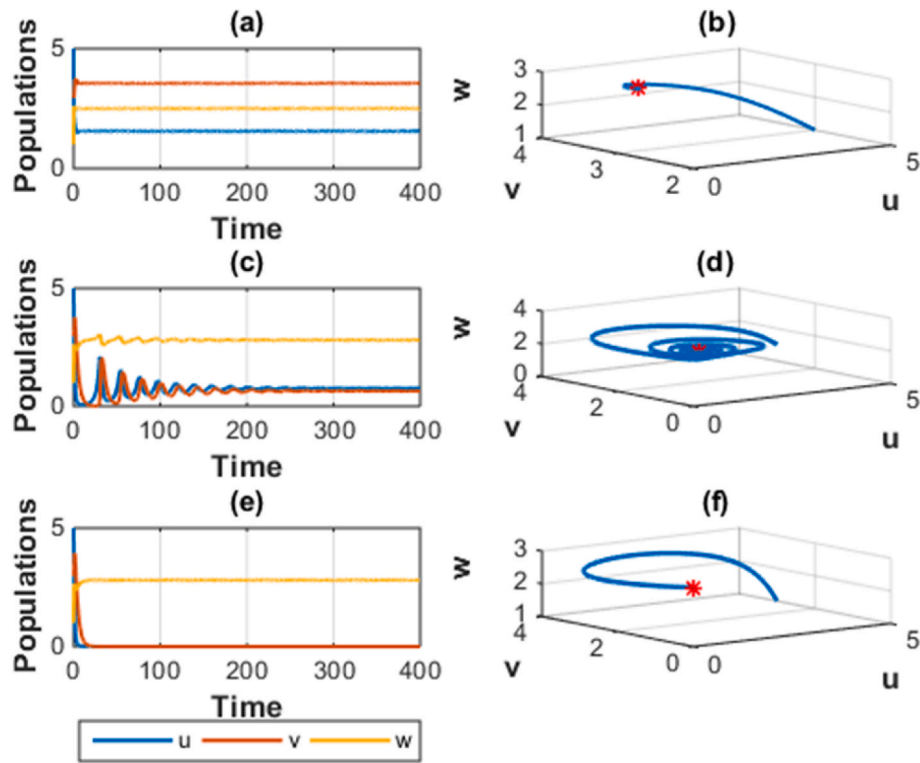


Fig. 7. (a) Time series of the DOPZ system with $r = 0.9$; (b) phase diagram corresponding to (a); (c) time series with $r = 0.1$; (d) phase diagram of (c); (e) time series with $r = 0.01$; (f) phase diagram of (e).

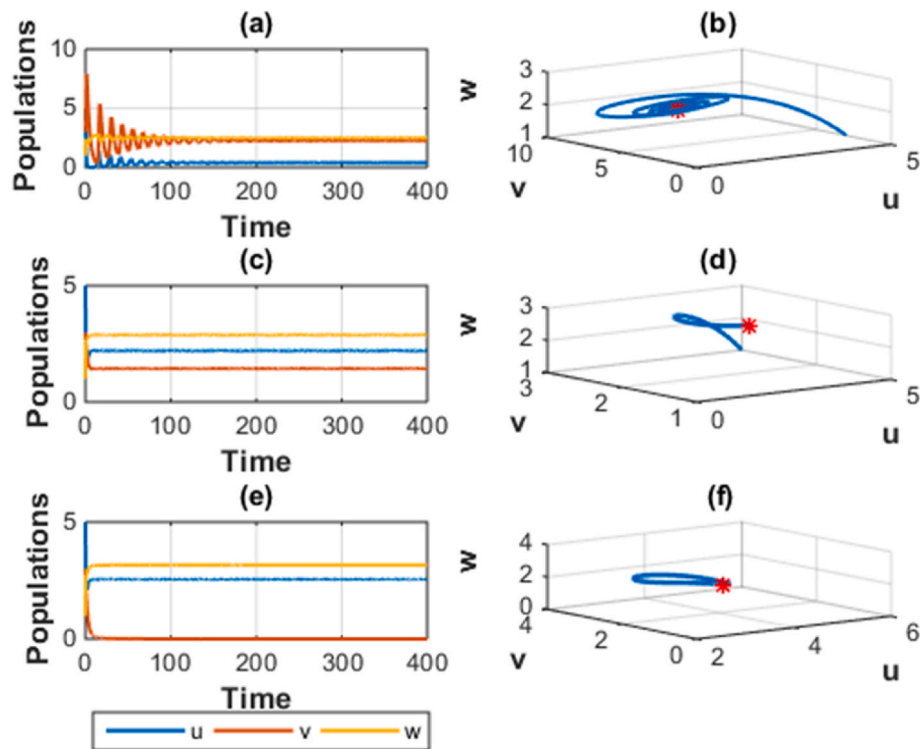


Fig. 8. (a) Time series of the DOPZ system with $\alpha_2 = 0.9$; (b) phase diagram corresponding to (a); (c) time series with $\alpha_2 = 0.1$; (d) phase diagram of (c); (e) time series with $\alpha_2 = 0.01$; (f) phase diagram of (e).

phytoplankton to zooplankton α_2 on the behaviour of the DOPZ system. The solution asymptotically approaches the CEP for $\alpha_2 \geq 0.1$, while the solution converges to the ZFEP in the uw -plane F_2 in $\text{Int. } R_{+(uw)}^2$ when

$\alpha_2 < 0.1$. This means that F_2 loses stability at $\alpha_2 = 0.1$. As a consequence, the outcome that was given by Theorem 4 has been demonstrated to be accurate by the numerical simulations.

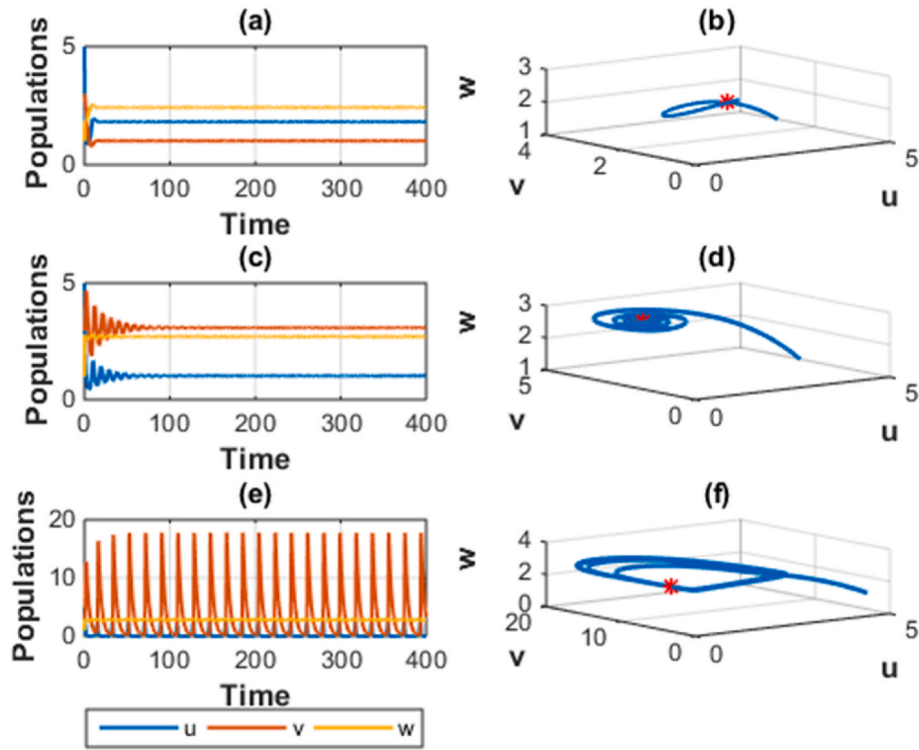


Fig. 9. (a) Time series of the DOPZ system with $\gamma_2 = 0.9$; (b) phase diagram corresponding to (a); (c) time series with $\gamma_2 = 0.1$; (d) phase diagram of (c); (e) time series with $\gamma_2 = 0.01$; (f) phase diagram of (e).

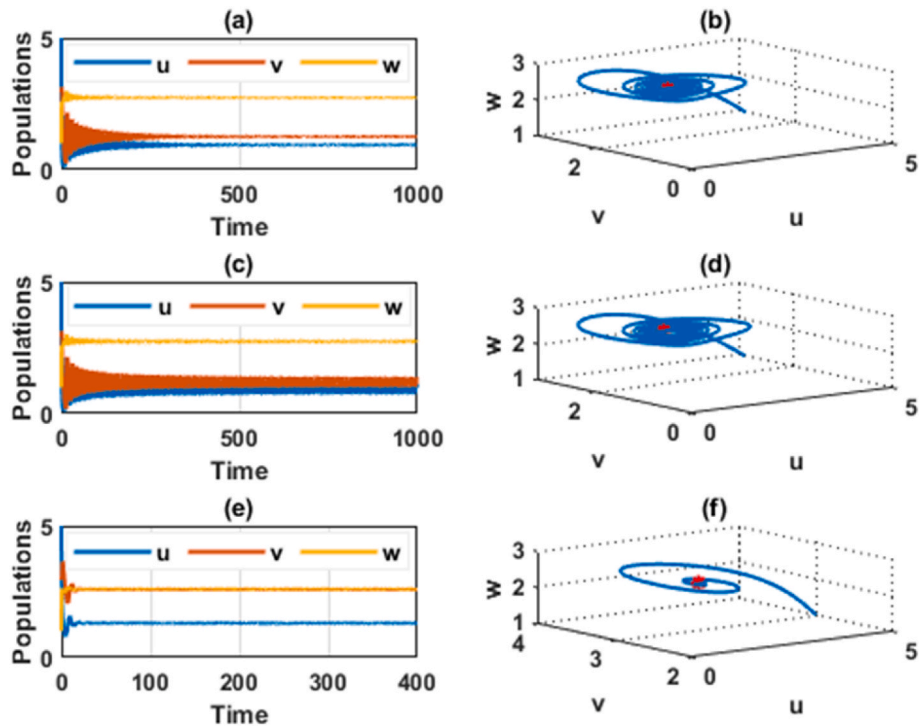


Fig. 10. (a) Time series of the DOPZ system with $\delta_1 = 0.67$; (b) phase diagram corresponding to (a); (c) time series with $\delta_1 = 0.68$; (d) phase diagram of (c); (e) time series with $\delta_1 = 0.0001$; (f) phase diagram of (e).

In addition, Fig. 9 displays the influence of varying the consumption of oxygen by zooplankton (γ_2). Clearly, the solution approaches the CEP level when $\gamma_2 \geq 0.1$. Further, for $\gamma_2 < 0.1$, the solution becomes a periodic attractor.

Now, Fig. 10 discusses the effect of changing δ_1 on the behaviour of

the DOPZ. The simulation shows for $\delta_1 \leq 0.67$, the solution accesses its CEP level. Further, for $\delta_1 > 0.67$, the solution encounters a periodic attractor.

Next, the influence of changing δ_2 is investigated in Fig. 11. The simulation illustrates that for $\delta_2 \geq 0.13$, the solution stabilizes at its CEP

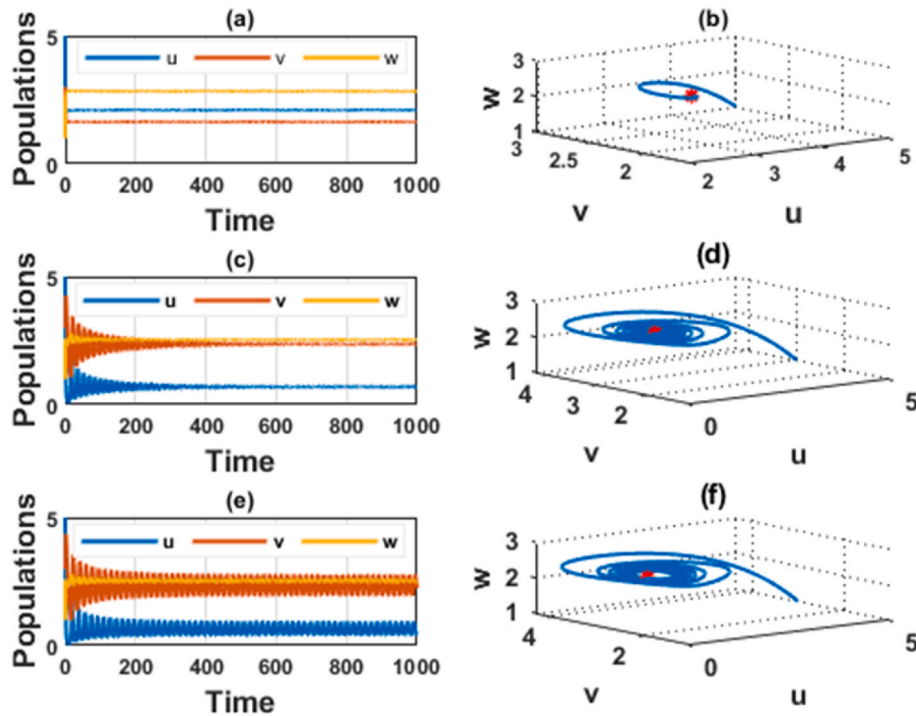


Fig. 11. (a) Time series of the DOPZ system with $\delta_2 = 0.9$; (b) phase diagram corresponding to (a); (c) time series with $\delta_2 = 0.13$; (d) phase diagram of (c); (e) time series with $\delta_2 = 0.129$; (f) phase diagram of (e).

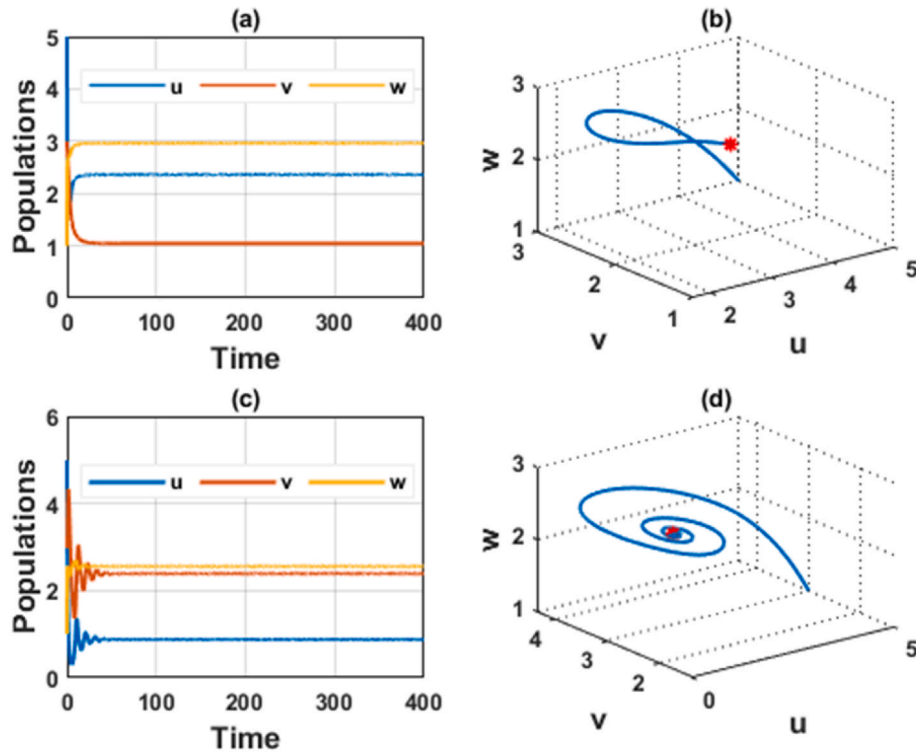


Fig. 12. (a) Time series of the DOPZ system with $a_2 = 0.9$; (b) phase diagram corresponding to (a); (c) time series with $a_2 = 0.001$; (d) phase diagram of (c).

level, while for $\delta_2 < 0.13$ the solution follows a periodic attractor.

Finally, for varying the following parameters each time $\alpha_1, s, d, m, a, \gamma, \alpha_1$ and a_2 , the solution approaches its CEP in the interior of $R^3_{(u,v,w)}$. For instance, see Fig. 12.

4. Discussion

This paper modified the dissolved oxygen-plankton model to include a strong Allee effect in the phytoplankton population taking into account that the zooplankton feeds on both toxic and non-toxic phytoplankton. The idea is to figure out how this kind of growth affects the dynamics of

an aquatic environment. The system underwent theoretical and numerical analysis. The theoretical results detect that there are three steady states; the first one is the dissolved oxygen equilibrium point DOEP which always has stable behaviour. The second one is the zooplankton-free equilibrium point ZFEP which shows stable behaviour under certain conditions; otherwise, it could have become unstable, leading to bifurcations of saddle-node or periodic nature. The third one is CEP which also could be stable or unstable depending on specific conditions. The essential conditions have been found to ensure the happening of different types of bifurcation around the ZFEP and CEP. Nonetheless, the numerical simulation deduced when the stability criteria are met, the DOPZ system always sways about the CEP. Further, changing the critical phytoplankton level k_0 (Allee threshold), the solution presents diverse dynamics, such as extinction only for the phytoplankton population, extinction for both plankton species, persistence of all components, or periodic attractor dynamics. Thus, it can be considered a critical parameter affecting the whole system's dynamics. Moreover, for large γ_1 , the consumption rate of oxygen by the phytoplankton during the night, and for small α_2 , the zooplankton population undergoes extinction, and so the solution of the DOPZ system is moved from the CEP to a ZFEP. In addition, for small r , the phytoplankton's growth rate, both phytoplankton and zooplankton populations face extinction. However, for small $\gamma_1, \gamma_2, \delta_2, w_0$, the DOPZ system shows limit cycle behaviour. The same behaviour could be detected for large δ_1 . Finally, the solution is stabilized at the CEP when the remaining parameters are changed.

5. Conclusion

The strong Allee effect type of growth term for the phytoplankton population was incorporated in this work. This seems necessary since phytoplankton, which is responsible for an estimated 50–80 % of the world's oxygen generation, is becoming more and more endangered because of the increase in waste thrown into the water, in particular industrial waste. This, in turn, leads to damage of the other marine species. Therefore, it is reasonable to ask: How could we avoid the extinction of phytoplankton? [Theorem 3](#) shows the conditions which guarantee that phytoplankton and zooplankton populations can coexist in a stable state. However, the simulation shows the system

demonstrates many phenomena such as coexistence, extinction, and the limit cycle by altering the parametric values. These phenomena are fundamental characteristics of non-linear models. Further, the simulation illustrations that if k_0 (Allee threshold of the phytoplankton population) and γ (The natural depletion rate of oxygen) cannot be controlled, the two species are threatened with extinction. For instance, the plankton population faces extinction at $k_0 \leq 0.001$, while zooplankton faces extinction for $0.001 < k_0 \leq 0.01$. For $0.01 < k_0 \leq 2$, the solution stabilized at the coexistence state. However, when $k_0 \geq 2.1$, the solution exhibits periodic attractor behaviour.

Finally, we suggest considering a stage structure for the zooplankton population in future work by expanding the model to include a system with four components. Further, the zooplankton population are assumed to grow logistically in the absence of the phytoplankton species, in this case, the latter is considered additional food for zooplankton.

Availability of data and materials

Data sharing is not applicable to this article as no data-sets were generated or analyzed during this study.

CRediT authorship contribution statement

Ahmed Ali: Writing – original draft, Resources, Investigation, Formal analysis, Conceptualization. **Shireen Jawad:** Writing – original draft, Methodology, Investigation, Formal analysis, Conceptualization. **Ali Hasan Ali:** Writing – review & editing, Visualization, Software, Methodology. **Matthias Winter:** Writing – review & editing, Supervision, Investigation, Formal analysis.

Declaration of competing interest

The authors declare that they have no known competing financial interests or personal relationships that could have appeared to influence the work reported in this paper.

Data availability

No data was used for the research described in the article.

Appendix

The coefficient of equation (2) is defined below as:

$$B_0 = a^2(am_1 - \gamma_1 m_2),$$

$$B_1 = 3a^2 m_1 m_3 + a^2 \gamma_1 m_2 m_4 + a^2 m_2 m_7 (d + \gamma_1) - a^3 m_5 - a^3 m_1 m_4 - 2am_2 m_6$$

$$B_2 = m_1 [2a_2^2 a - 4a_2 a^2 a_2 - 4a_2 a^2 w_0 + 3a^2 a_2^2 + 6a^3 a_2 w_0 + 2a^3 w_0^2 + a_2 a - 2a_2 a^2 a_2 - 2a_2 a^2 w_0 + a^3 w_0^2] - 3a^2 m_5 m_3 + a^3 m_4 m_5 \\ - 3a^2 m_1 m_3 m_4 + m_2 [2\gamma_1 m_6 m_4 - (\alpha_2 - 2a_2 am_7 + a^2 a_2^2 + 2a^2 a_2 w_0 + a^2 w_0) - a^2 m_4 + 2m_6 m_7 (d + \gamma) - a^2 dm_7] + \gamma_1 r \delta^2 + a(m_8 - m_9)$$

$$B_3 = m_1 [a_2^3 - 3a_2^2 aa_2 - 3a_2^2 aw_0 + 3a_2 a^2 a_2^2 + 6a_2 a^2 a_2 w_0 + 4a_2 a^2 w_0^2 - a^3 a_2^3 - 3a^3 a_2^2 w_0 - a^2 a_2 w_0^2 - 2a^3 a_2 w_0^2 + a^3 w_0^3] - m_5 [2a_2^2 a - 4a_2 a^2 a_2 \\ - 4a_2 a^2 w_0 + 3a^2 a_2^2 + 6a^3 a_2 w_0 + 2a^3 w_0^2 + a_2 a - 2a_2 a^2 a_2 - 2a_2 a^2 w_0 + a^3 w_0^2] + 3a^2 m_5 m_4 - m_1 m_4 [2a_2^2 a - 4a_2 a^2 a_2 \\ - 4a_2 a^2 w_0 + 3a^3 a_2^2 + 4a^3 a_2 w_0 + 2a^3 w_0^2 + a_2 a - 2a_2 a^2 a_2 - a_2 a^2 w_0 + 2a^3 a_2 w_0 + a^3 w_0^3] + m_2 [\gamma_1 m_4 (\alpha_2 - 2a_2 aa_2 - 2a_2 aw_0 + a^2 a_2^2 + 2a^2 a_2 w_0 + a^2 w_0) \\ - 2am_3 m_4 - (\alpha_2 - 2a_2 aa_2 - 2a_2 aw_0 + a^2 a_2^2 + 2a^2 a_2 w_0 + a^2 w_0)(d + \gamma_1)m_7 + (a^2 m_4 - 2am_3)(dm_7)] - 2\gamma_1 r \delta^2 m_7 - m_8 (2am_7 - a_2) + m_9 (ra + \delta_1 am_4 \\ - \alpha_2 + am_7) B_4 = m_4 m_5 [2a_2^2 a - 4a_2 a^2 a_2 - 4a_2 a^2 w_0 + 3a^2 a_2^2 + 6a^3 a_2 w_0 + 2a^3 w_0^2 + a_2 a - 2a_2 a^2 a_2 - 2a_2 a^2 w_0 + a^3 w_0^2] - m_5 [a_2^3 - 3a_2^2 aa_2 \\ - 3a_2^2 aw_0 + 3a_2 a^2 a_2^2 + 6a_2 a^2 a_2 w_0 + 4a_2 a^2 w_0^2 - a^3 a_2^3 - 3a^3 a_2^2 w_0 - a^2 a_2 w_0^2 - 2a^3 a_2 w_0^2 + a^3 w_0^3] - m_1 m_4 [a_2^3 - 3a_2^2 aa_2 \\ - 3a_2^2 aw_0 + 3a_2 a^2 a_2^2 + 6a_2 a^2 a_2 w_0 + 4a_2 a^2 w_0^2 - a^3 a_2^3 - 3a^3 a_2^2 w_0 - a^2 a_2 w_0^2 - 2a^3 a_2 w_0^2 + a^3 w_0^3] + m_2 [2am_3 m_4 - dm_7 (\alpha_2 - 2a_2 aa_2 \\ - 2a_2 aw_0 + a^2 a_2^2 + 2a^2 a_2 w_0 + a^2 w_0) - (\alpha_2 - 2a_2 aa_2 - 2a_2 aw_0 + a^2 a_2^2 + 2a^2 a_2 w_0 + a^2 w_0^2)(dm_4 + \gamma_1 m_4 m_7)] + \gamma_1 r \delta_1^2 m_7^2 - m_7 (\alpha_2 m_8 + am_7) + m_9 (ra_2 \\ - ram_7 + \delta_1 a_2 m_4 - a \delta_1 m_4 m_7)$$

$$B_5 = m_4 m_5 [a_2^3 - 3a_2^2 a a_2 - 3a_2^2 a w_0 + 3a_2 a^2 a_2^2 + 6a_2 a^2 a_2 w_0 + 4a_2 a^2 w_0 - a^3 a_2^3 - 3a^3 a_2^3 w_0 - a^2 a_2 w_0^2 - 2a^3 a_2 w_0^2 + a^3 w_0^3] + m_2 m_4 m_7 d (a_2 - 2a_2 a a_2 - 2a_2 a w_0 + a^2 a_2^2 + 2a^2 a_2 w_0 + a^2 w_0^2).$$

Here $m_1 = (s + \gamma)(1 - m)^4 \alpha_1 k k_0$, $m_2 = \delta_1 \alpha_1 k k_0 (1 - m)^3$, $m_3 = a_2 - a a_2 - a w_0$, $m_4 = a_1 + w_0$, $m_5 = s w_0 \alpha_1 k k_0 (1 - m)^4$, $m_6 = a_2 a - a a_2^2 - a^2 w_0$, $m_7 = a_2 + w_0$, $m_8 = r \gamma_1 \delta_1 (k + k_0)(1 - m)$, $m_9 = \gamma_1 k k_0 (1 - m)$.

References

- [1] V. Hull, L. Parrella, M. Falcucci, Modelling dissolved oxygen dynamics in coastal lagoons, *Ecol. Model.* 211 (3–4) (2008) 468–480.
- [2] A.K. Misra, Modeling the depletion of dissolved oxygen in a lake due to submerged macrophytes, *Nonlinear Anal. Model Control* 15 (2) (2010) 185–198.
- [3] A.K. Misra, P. Chandra, V. Raghavendra, Modeling the depletion of dissolved oxygen in a lake due to algal bloom: effect of time delay, *Adv. Water Resour.* 34 (10) (2011) 1232–1238.
- [4] Y. Sekerci, S. Petrovskii, Mathematical modelling of plankton–oxygen dynamics under the climate change, *Bull. Math. Biol.* 77 (12) (2015) 2325–2353.
- [5] K. Hancke, R.N. Glud, Temperature effects on respiration and photosynthesis in three diatom-dominated benthic communities, *Aquat. Microb. Ecol.* 37 (3) (2004) 265–281.
- [6] S. Mandal, S. Ray, P.B. Ghosh, Modeling nutrient (dissolved inorganic nitrogen) and plankton dynamics at Sagar island of Hooghly–Matla estuarine system, West Bengal, India, *Nat. Resour. Model.* 25 (4) (2012) 629–652.
- [7] A. Gökçe, A mathematical study for chaotic dynamics of dissolved oxygen–phytoplankton interactions under environmental driving factors and time lag, *Chaos, Solit. Fractals* 151 (2021) 111268.
- [8] H. Hao, R. Mo, S. Kang, Z. Wu, Effects of temperature, inlet gas pressure and humidity on PEM water contents and current density distribution, *Results Eng* 20 (2023) 101411.
- [9] S. Mandal, G. Samanta, M. De la Sen, Dynamics of oxygen–Plankton model with variable zooplankton search rate in deterministic and fluctuating environments, *Mathematics* 10 (10) (2022) 1641.
- [10] S.M. Salman, A.A. Elsadany, Higher order codimension bifurcations in a discrete-time toxic-phytoplankton–zooplankton model with Allee effect, *Int. J. Nonlinear Sci. Numer. Stimul.* 24 (5) (2022) 1631–1658.
- [11] M.S. Surendar, M. Sambath, Qualitative analysis for a phytoplankton–zooplankton model with allee effect and holling type II response, *Discontinuity, Nonlinearity, Complex.* 10 (1) (2021) 1–18.
- [12] Q. Lin, Allee effect increasing the final density of the species subject to the Allee effect in a Lotka–Volterra commensal symbiosis model, *Adv. Differ. Equ.* 2018 (1) (2018) 1–9.
- [13] X. Pan, M. Zhao, Y. Wang, H. Yu, Z. Ma, Q. Wang, Stability and dynamical analysis of a biological system, in: *Abstract and Applied Analysis*, vol. 2014, 2014.
- [14] S.R. Jawad, M. Al Nuaimi, Persistence and bifurcation analysis among four species interactions with the influence of competition, predation and harvesting, *Iraqi J. Sci.* (2023) 1369–1390.
- [15] S. Dawud, S. Jawad, Stability analysis of a competitive ecological system in a polluted environment, *Commun. Math. Biol. Neurosci.* 2022 (2022).
- [16] M. Al Nuaimi, S. Jawad, Modelling and stability analysis of the competition ecological model with harvesting, *Commun. Math. Biol. Neurosci.* 2022 (2022).
- [17] S. K. Sasmal Sajan, B. Dubey, A phytoplankton–zooplankton–fish model with chaos control: in the presence of fear effect and an additional food, *Chaos An Interdiscip. J. Nonlinear Sci.* 32 (1) (2022) 13114.
- [18] A. Vodenikov, V. Melnikova, A. Minibaev, N. Lazarev, Control of condensate dissolved oxygen in steam surface condenser. Reconstruction experience, *Results Eng* 15 (2022) 100492.
- [19] X.-Y. Meng, L. Xiao, Stability and bifurcation for a delayed diffusive two-zooplankton one-phytoplankton model with two different functions, *Complexity* 2021 (2021).
- [20] T.G. Hallam, C.E. Clark, G.S. Jordan, Effects of toxicants on populations: a qualitative approach II. First order kinetics, *J. Math. Biol.* 18 (1) (1983) 25–37.
- [21] S. Chakraborty, S. Chatterjee, E. Venturino, J. Chattopadhyay, Recurring plankton bloom dynamics modeled via toxin-producing phytoplankton, *J. Biol. Phys.* 33 (4) (2007) 271–290.
- [22] J. Dhar, R.S. Baghel, Role of dissolved oxygen on the plankton dynamics in spatio-temporal domain, *Model. Earth Syst. Environ.* 2 (1) (2016) 1–15.
- [23] V.P. Dubey, J. Singh, A.M. Alshehri, S. Dubey, D. Kumar, Numerical investigation of fractional model of phytoplankton–toxic phytoplankton–zooplankton system with convergence analysis, *Int. J. Biomath. (IJB)* 15 (4) (2022) 2250006.
- [24] L. Niu, Q. Chen, Z. Teng, Bifurcation analysis in a discrete toxin-producing phytoplankton–zooplankton model with refuge, *J. Differ. Equations Appl.* (2024) 1–26.
- [25] R. Chandra, P. Gupta, A. Priyadarshi, Holling type-II functional response in aquatic ecosystem models shaping spatial heterogeneous distribution of Phytoplankton data at Tokyo Bay, *AIP Conf. Proc.* 3087 (1) (2024).
- [26] W. Zhang, S. Han, D. Zhang, B. Shan, D. Wei, Variations in dissolved oxygen and aquatic biological responses in China’s coastal seas, *Environ. Res.* 223 (2023) 115418.
- [27] M.W. Hirsch, S. Smale, R.L. Devaney, *Differential Equations, Dynamical Systems, and an Introduction to Chaos*, Academic press, 2012.
- [28] P. Hartman, *Ordinary Differential Equations*, second ed., SIAM, Philadelphia, PA, 2002.
- [29] A.K. Paul, N. Basak, M.A. Kuddus, Mathematical analysis and simulation of COVID-19 model with booster dose vaccination strategy in Bangladesh, *Results Eng* 21 (2024) 101741.
- [30] J.H. Hubbard, B.H. West, *Differential Equations: A Dynamical Systems Approach: Ordinary Differential Equations*, vol. 5, Springer, 2013.
- [31] L. Perko, *Differential Equations and Dynamical Systems*, vol. 7, Springer Science & Business Media, 2013.
- [32] J.P. LaSalle, Stability theory and invariance principles, in: *Dynamical Systems*, Elsevier, 1976, pp. 211–222.
- [33] R.M. May, *Stability and Complexity in Model Ecosystems*, Princeton university press, 2019.
- [34] Z.U. Rehman, Z. Hussain, Z. Li, T. Abbas, I. Tlili, Bifurcation analysis and multi-stability of chirped form optical solitons with phase portrait, *Results Eng* (2024) 101861.
- [35] Y.A. Kuznetsov, *Elements of Applied Bifurcation Theory*, vol. 112, Springer Science & Business Media, 2013.
- [36] D. Mukherjee, Study of fear mechanism in predator–prey system in the presence of competitor for the prey, *Ecol. Genet. Genomics* 15 (2020) 100052.
- [37] A.A. Yinusa, M.G. Sobamowo, A.O. Adelaja, Thermal analysis of nanofluidic flow through multi-walled carbon nanotubes subjected to perfectly and imperfectly bonded wall conditions, *Chem. Thermodyn. Therm. Anal.* 5 (2022) 100028.
- [38] M. Al-Raeei, Morse potential specific bond volume: a simple formula with applications to dimers and soft–hard slab slider, *J. Phys. Condens. Matter* 34 (28) (2022) 284001.
- [39] M.A.E. Abdelrahman, A. Alharbi, Analytical and numerical investigations of the modified Camassa–Holm equation, *Pramana* 95 (2021) 1–9.
- [40] A.A. Thirthar, P. Panja, A. Khan, M.A. Alqudah, An ecosystem model with memory effect considering global warming, *J. Theor. Biol.* 419 (2017) 13–22.
- [41] S.K. Hassan, S.R. Jawad, The effect of mutual interaction and harvesting on food chain model, *Iraqi J. Sci.* (2022) 2641–2649.